

# CITATION REPORT

List of articles citing

## Origin of apparent colossal dielectric constants

DOI: 10.1103/physrevb.66.052105  
Physical Review B, 2002, 66, .

**Source:** <https://exaly.com/paper-pdf/34065597/citation-report.pdf>

**Version:** 2024-04-25

This report has been generated based on the citations recorded by exaly.com for the above article. For the latest version of this publication list, visit the link given above.

The third column is the impact factor (IF) of the journal, and the fourth column is the number of citations of the article.

#	Paper	IF	Citations
778	Synthesis and Characterisation of B-Site Doped Cu <sub>2</sub> Ta <sub>4</sub> O <sub>12</sub> . <b>2002</b> , 755, 1		
777	Deposition and dielectric properties of CaCu <sub>3</sub> Ti <sub>4</sub> O <sub>12</sub> thin films on Pt/Ti/SiO <sub>2</sub> /Si substrates using pulsed-laser deposition. <i>Thin Solid Films</i> , <b>2003</b> , 440, 60-65	2.2	66
776	Lattice dielectric response of CdCu <sub>3</sub> Ti <sub>4</sub> O <sub>12</sub> and CaCu <sub>3</sub> Ti <sub>4</sub> O <sub>12</sub> from first principles. <i>Physical Review B</i> , <b>2003</b> , 67,	3.3	86
775	Dielectric properties and dynamical conductivity of LaTiO <sub>3</sub> : From dc to optical frequencies. <i>Physical Review B</i> , <b>2003</b> , 68,	3.3	48
774	Charge transfer in the high dielectric constant materials CaCu <sub>3</sub> Ti <sub>4</sub> O <sub>12</sub> and CdCu <sub>3</sub> Ti <sub>4</sub> O <sub>12</sub> . <i>Physical Review B</i> , <b>2003</b> , 67,	3.3	157
773	Response of disordered matter to electromagnetic fields. <b>2003</b> , 91, 207601		129
772	Extrinsic models for the dielectric response of CaCu <sub>3</sub> Ti <sub>4</sub> O <sub>12</sub> . <i>Journal of Applied Physics</i> , <b>2003</b> , 94, 3299-3306		295
771	Focusing of millimeter-wave radiation beyond the Abbe barrier. <b>2003</b> , 83, 4122-4124		14
770	Electronic and optical properties of LiBC. <i>Physical Review B</i> , <b>2003</b> , 67,	3.3	14
769	The many surprises of ferroelectric superlattices. <i>Journal of Physics Condensed Matter</i> , <b>2003</b> , 15, V11-V12.8		19
768	Ionic, Dipolar, and Interfacial Processes. <b>2004</b> , 753-759		
767	Broad-band dielectric spectroscopy of SrTiO <sub>3</sub> :Bi ceramics. <i>Physical Review B</i> , <b>2004</b> , 69,	3.3	31
766	Effects of postanneal conditions on the dielectric properties of CaCu <sub>3</sub> Ti <sub>4</sub> O <sub>12</sub> thin films prepared on Pt/Ti/SiO <sub>2</sub> /Si substrates. <i>Journal of Applied Physics</i> , <b>2004</b> , 95, 6483-6485	2.5	92
765	Structural characteristics of epitaxial BaTiO <sub>3</sub> /LaNiO <sub>3</sub> superlattice. <i>Journal of Applied Physics</i> , <b>2004</b> , 96, 584-589	2.5	40
764	High permittivity Li and Al doped NiO ceramics. <b>2004</b> , 85, 5664-5666		73
763	Dielectric responses of the layered cobalt oxysulfide Sr <sub>2</sub> Cu <sub>2</sub> CoO <sub>2</sub> S <sub>2</sub> with CoO <sub>2</sub> square planes. <i>Journal of Applied Physics</i> , <b>2004</b> , 95, 6816-6818	2.5	6
762	Maxwell-Wagner effect in hexagonal BaTiO <sub>3</sub> single crystals grown by containerless processing. <b>2004</b> , 85, 2899-2901		42

761	Effect of mechanical deformation on the critical current in YBa <sub>2</sub> Cu <sub>3</sub> O <sub>7-<math>\delta</math></sub> superconducting films. <b>2004</b> , 49, 512-515		
760	Giant piezoelectric and dielectric enhancement in disordered heterogeneous systems. <b>2004</b> , 46, 2213-2216		12
759	X-ray reflectivity study of the structural characteristics of BaTiO <sub>3</sub> /LaNiO <sub>3</sub> superlattice. <i>Thin Solid Films</i> , <b>2004</b> , 469-470, 500-504	2.2	15
758	Electric and dielectric properties of pure and doped CaCu <sub>3</sub> Ti <sub>4</sub> O <sub>12</sub> perovskite materials. <b>2004</b> , 132, 241-246		134
757	Influence of charge-ordering on the dielectric response of La <sub>1-x</sub> Sr <sub>x</sub> MnO <sub>3</sub> . <b>2004</b> , 323, 473-476		16
756	Giant dielectric permittivity caused by carrier hopping in a layered cuprate Bi <sub>2</sub> Ba <sub>2</sub> Nd <sub>1.6</sub> Ce <sub>0.4</sub> Cu <sub>2</sub> O <sub>10+<math>\delta</math></sub> . <b>2004</b> , 333, 450-456		2
755	Temperature dependent total scattering structural study of CaCu <sub>3</sub> Ti <sub>4</sub> O <sub>12</sub> . <i>Journal of Physics Condensed Matter</i> , <b>2004</b> , 16, S5091-S5102	1.8	29
754	Dielectric response of the charge-ordered two-dimensional nickelate La <sub>1.5</sub> Sr <sub>0.5</sub> NiO <sub>4</sub> . <b>2004</b> , 85, 6224-6226		65
753	Disordered Ferroelectric Systems: Giant Dielectric Enhancement, Maxwell-Wagner Relaxations and Conductor-Insulator Transition. <b>2004</b> , 307, 171-176		2
752	Characterization and dielectric properties of polyaniline-TiO <sub>2</sub> nanocomposites. <b>2004</b> , 15, 1277-1283		238
751	Dielectric behavior of copper tantalum oxide. <i>Journal of Applied Physics</i> , <b>2004</b> , 96, 4400-4404	2.5	58
750	Large dielectric constant and Maxwell-Wagner relaxation in Bi <sub>2</sub> B <sub>1-x</sub> Cu <sub>3</sub> Ti <sub>4</sub> O <sub>12</sub> . <i>Physical Review B</i> , <b>2004</b> , 70,	3.3	411
749	Polaron relaxation and variable-range-hopping conductivity in the giant-dielectric-constant material CaCu <sub>3</sub> Ti <sub>4</sub> O <sub>12</sub> . <i>Physical Review B</i> , <b>2004</b> , 70,	3.3	309
748	Evidence for power-law frequency dependence of intrinsic dielectric response in the CaCu <sub>3</sub> Ti <sub>4</sub> O <sub>12</sub> . <i>Physical Review B</i> , <b>2004</b> , 70,	3.3	103
747	Dielectric response of sputtered transition metal oxides. <i>Journal of Applied Physics</i> , <b>2004</b> , 95, 8087-8091	2.5	24
746	Low-temperature permittivity of insulating perovskite manganites. <i>Physical Review B</i> , <b>2004</b> , 70,	3.3	69
745	Nonintrinsic origin of the colossal dielectric constants in CaCu <sub>3</sub> Ti <sub>4</sub> O <sub>12</sub> . <i>Physical Review B</i> , <b>2004</b> , 70,	3.3	551
744	Phase-Transition and Dynamics of Ferroelectric-Paraelectric Multilayer Structure. <b>2004</b> , 300, 131-134		

743	Dielectric studies in a layered Ba based Bi-2222 cuprate $\text{Bi}_2\text{Ba}_2\text{Nd}_{1.6}\text{Ce}_{0.4}\text{Cu}_2\text{O}_{10}$ □ <b>2005</b> , 417, 166-170		29
742	Mechanism for Developing the Boundary Barrier Layers of $\text{CaCu}_3\text{Ti}_4\text{O}_{12}$ . <i>Journal of the American Ceramic Society</i> , <b>2005</b> , 87, 2072-2079	3.8	247
741	Relaxor ferroelectricity and colossal magnetocapacitive coupling in ferromagnetic $\text{CdCr}_2\text{S}_4$ . <b>2005</b> , 434, 364-7		437
740	Polarization of High-Permittivity Dielectric NiO-Based Ceramics. <i>Journal of the American Ceramic Society</i> , <b>2005</b> , 88, 1808-1811	3.8	33
739	The electrode/sample contact effects on the dielectric properties of the $\text{CaCu}_3\text{Ti}_4\text{O}_{12}$ ceramic. <b>2005</b> , 59, 3990-3993		48
738	Dielectric response in the charge-ordered $\text{Ca}_2\text{Pr}_x\text{MnO}_4$ phases. <b>2005</b> , 7, 905-911		18
737	Microstructure and dielectric properties of pulsed-laser-deposited $\text{CaCu}_3\text{Ti}_4\text{O}_{12}$ thin films on $\text{LaNiO}_3$ buffered Pt/Ti/SiO <sub>2</sub> /Si substrates. <i>Applied Physics A: Materials Science and Processing</i> , <b>2005</b> , 80, 1763-1767	2.6	19
736	Effects of Processing Conditions on the Dielectric Properties of $\text{CaCu}_3\text{Ti}_4\text{O}_{12}$ . <b>2005</b> , 15, 203-208		28
735	High Dielectric Constant in the Charge-ordered Manganese Oxide $\text{CaMn}_7\text{O}_{12}$ . <b>2005</b> , 631, 2192-2196		14
734	Study of the Dielectric Properties of the Perovskite $\text{LaMn}_{0.5}\text{Co}_{0.5}\text{O}_3$ □ <b>2005</b> , 631, 2265-2272		34
733	Preparation of core/shell structured NiO-based ceramics and their dielectric properties. <b>2005</b> , 38, 1615-1620		8
732	Relaxation dynamics and colossal magnetocapacitive effect in $\text{CdCr}_2\text{S}_4$ . <i>Physical Review B</i> , <b>2005</b> , 72, 3-3	3.3	48
731	Colossal dielectric and electromechanical responses in self-assembled polymeric nanocomposites. <b>2005</b> , 87, 182901		64
730	Giant barrier layer capacitance effects in the lithium ion conducting material $\text{La}_{0.67}\text{Li}_{0.25}\text{Ti}_{0.75}\text{Al}_{0.25}\text{O}_3$ . <b>2005</b> , 86, 043110		23
729	Origin of the colossal permittivity and possible application of CCT ceramics.		1
728	Effective Dielectric Function in High-Permittivity Ceramics and Films. <b>2005</b> , 316, 89-95		14
727	High-permittivity core/shell structured NiO-based ceramics and their dielectric response mechanism. <i>Physical Review B</i> , <b>2005</b> , 72, 3-3	3.3	79
726	High dielectric constant in $\text{CaCu}_{3/\text{sub}}\text{Ti}_{4/\text{sub}}\text{O}_{12}$ / multiphased ceramics. <b>2005</b> ,		

725	The effect of SiO <sub>2</sub> barrier layer on the dielectric properties of CaCu <sub>3</sub> Ti <sub>4</sub> O <sub>12</sub> films. <b>2005</b> , 38, 4236-4240		18
724	Magnetodielectric consequences of phase separation in the colossal magnetoresistance manganite Pr <sub>0.7</sub> Ca <sub>0.3</sub> MnO <sub>3</sub> . <i>Physical Review B</i> , <b>2005</b> , 72,	3-3	74
723	Intrinsic dielectric properties and charge transport in oligomers of organic semiconductor copper phthalocyanine. <i>Physical Review B</i> , <b>2005</b> , 71,	3-3	33
722	Glassy freezing of orbital dynamics in FeCr <sub>2</sub> S <sub>4</sub> and FeSc <sub>2</sub> S <sub>4</sub> . <b>2005</b> , 351, 2793-2797		11
721	Dielectric properties and Maxwell-Wagner relaxation of compounds ACu <sub>3</sub> Ti <sub>4</sub> O <sub>12</sub> (A=Ca, Bi <sub>2</sub> B, Y <sub>2</sub> B, La <sub>2</sub> B). <i>Journal of Applied Physics</i> , <b>2005</b> , 98, 093703	2-5	241
720	Dielectric and magnetic properties of Fe- and Nb-doped CaCu <sub>3</sub> Ti <sub>4</sub> O <sub>12</sub> . <i>Physical Review B</i> , <b>2005</b> , 72,	3-3	149
719	Origin of the colossal dielectric response of Pr <sub>0.6</sub> Ca <sub>0.4</sub> MnO <sub>3</sub> . <i>Physical Review B</i> , <b>2005</b> , 72,	3-3	110
718	Electrode and grain-boundary effects on the conductivity of CaCu <sub>3</sub> Ti <sub>4</sub> O <sub>12</sub> . <b>2005</b> , 87, 022907		94
717	Giant dielectric permittivity of electron-doped manganite thin films, Ca <sub>1-x</sub> La <sub>x</sub> MnO <sub>3</sub> (0<x<0.03). <i>Journal of Applied Physics</i> , <b>2005</b> , 97, 034102	2-5	34
716	Dielectric dispersion of CaCu <sub>3</sub> Ti <sub>4</sub> O <sub>12</sub> ceramics at high temperatures. <b>2005</b> , 87, 142901		155
715	Novel dielectric anomaly in the hole-doped La <sub>2</sub> Cu <sub>1-x</sub> Li <sub>x</sub> O <sub>4</sub> and La <sub>2-x</sub> Sr <sub>x</sub> NiO <sub>4</sub> insulators: signature of an electronic glassy state. <b>2005</b> , 94, 017002		87
714	Evidence of the Internal Domains for Inducing the Anomalously High Dielectric Constant of CaCu <sub>3</sub> Ti <sub>4</sub> O <sub>12</sub> . <b>2005</b> , 17, 5167-5171		239
713	Structural, Electrical and Dielectric Properties of Uranium Doped Barium Titanate. <b>2006</b> , 514-516, 1269-1273		
712	CaCu <sub>3</sub> Ti <sub>4</sub> O <sub>12</sub> : Low-Temperature Synthesis by Pyrolysis of an Organic Solution. <b>2006</b> , 18, 3878-3882		77
711	Polarizability of phthalocyanine based molecular systems: A first-principles electronic structure study. <b>2006</b> , 88, 222903		26
710	Dielectric properties of doping-free NaMn <sub>7</sub> O <sub>12</sub> : Origin of the observed colossal dielectric constant. <i>Physical Review B</i> , <b>2006</b> , 74,	3-3	18
709	Increase of the Dielectric Constant near a Magnetic Transition in La <sub>0.5</sub> Ca <sub>0.5</sub> MnO <sub>3</sub> . <b>2006</b> ,		
708	Scaling of terahertz conductivity at the metal-insulator transition in doped manganites. <i>Physical Review B</i> , <b>2006</b> , 73,	3-3	11

707	Role of oxygen vacancies in the magnetic and dielectric properties of the high-dielectric-constant system CaCu <sub>3</sub> Ti <sub>4</sub> O <sub>12</sub> : An electron-spin resonance study. <i>Physical Review B</i> , <b>2006</b> , 73,	3.3	59
706	Giant dielectric response in the one-dimensional charge-ordered semiconductor (NbSe <sub>4</sub> ) <sub>3</sub> I. <b>2006</b> , 96, 046402		21
705	High-pressure x-ray diffraction study of the giant dielectric constant material CaCu <sub>3</sub> Ti <sub>4</sub> O <sub>12</sub> : Evidence of stiff grain surface. <b>2006</b> , 88, 191903		10
704	Multiferroic properties of Pb(Zr,Ti)O <sub>3</sub> /CoFe <sub>2</sub> O <sub>4</sub> composite thin films. <i>Journal of Applied Physics</i> , <b>2006</b> , 100, 126105	2.5	94
703	Elastic Constants Relaxation in Disordered Heterogeneous Systems. <b>2006</b> , 115, 215-220		
702	Colossal magnetocapacitance and colossal magnetoresistance in HgCr <sub>2</sub> S <sub>4</sub> . <b>2006</b> , 96, 157202		129
701	Dielectric properties of the charge-ordered mixed oxide CaMn <sub>7</sub> O <sub>12</sub> . <i>Journal of Physics Condensed Matter</i> , <b>2006</b> , 18, 3803-3815	1.8	14
700	Magnetic-field-dependent dielectric constant in La <sub>2</sub> B <sub>1</sub> Ca <sub>1</sub> MnO <sub>3</sub> . <b>2006</b> , 88, 242906		39
699	Analysis of Electrical Properties of Post-Annealed Polycrystalline CaCu <sub>3</sub> Ti <sub>4</sub> O <sub>12</sub> Films by Impedance Spectroscopy. <b>2006</b> , 23, 990-993		3
698	Microstructure and electrical properties of CaCu <sub>3</sub> Ti <sub>4</sub> O <sub>12</sub> ceramics. <i>Journal of Applied Physics</i> , <b>2006</b> , 99, 084106	2.5	175
697	The intrinsic conductivity of nanosized semiconducting crystals. <b>2006</b> , 3, 259-262		5
696	Decrease of dielectric loss in CaCu <sub>3</sub> Ti <sub>4</sub> O <sub>12</sub> ceramics by La doping. <i>Physica Status Solidi (A) Applications and Materials Science</i> , <b>2006</b> , 203, R22-R24	1.6	90
695	Growth of highly-oriented CaCu <sub>3</sub> Ti <sub>4</sub> O <sub>12</sub> thin films on SrTiO <sub>3</sub> (1 0 0) substrates by a chemical solution route. <b>2006</b> , 253, 2268-2271		19
694	Phase coexistence in solid solutions. <b>2006</b> , 179, 2443-2451		15
693	Apparent giant dielectric constants, dielectric relaxation, and ac-conductivity of hexagonal perovskites La <sub>1.2</sub> Sr <sub>2.7</sub> B <sub>0.7</sub> O <sub>7.33</sub> (B=Ru, Ir). <b>2006</b> , 179, 3965-3973		41
692	Maxwell-Wagner characterization of dielectric relaxation in Ni <sub>0.8</sub> Zn <sub>0.2</sub> Fe <sub>2</sub> O <sub>4</sub> /Sr <sub>0.5</sub> Ba <sub>0.5</sub> Nb <sub>2</sub> O <sub>6</sub> composite. <b>2006</b> , 137, 120-125		68
691	Reduced dielectric loss and leakage current in CaCu <sub>3</sub> Ti <sub>4</sub> O <sub>12</sub> /SiO <sub>2</sub> /CaCu <sub>3</sub> Ti <sub>4</sub> O <sub>12</sub> multilayered films. <b>2006</b> , 137, 381-386		42
690	Magnetic and transport and dielectric properties of polycrystalline TbMnO <sub>3</sub> . <b>2006</b> , 138, 481-484		34

689	On dielectric spectra of thin copper phthalocyanine films. <i>Thin Solid Films</i> , <b>2006</b> , 514, 287-291	2.2	11
688	Magnetocapacitance without magnetoelectric coupling. <b>2006</b> , 88, 102902		710
687	Dielectric spectra of disordered ferroelectric systems: Polycrystals and composites. <b>2006</b> , 48, 1157-1159		9
686	Multiferroic behavior in CdCr <sub>2</sub> X <sub>4</sub> (X=S,Se). <i>Physica B: Condensed Matter</i> , <b>2006</b> , 378-380, 363-366	2.8	21
685	Structural characterization of sputter-deposited Ba <sub>0.48</sub> Sr <sub>0.52</sub> TiO <sub>3</sub> /LaNiO <sub>3</sub> artificial superlattice structure by X-ray reflectivity and diffraction. <i>Thin Solid Films</i> , <b>2006</b> , 515, 1102-1106	2.2	3
684	Dynamic conductivity from audio to optical frequencies of semiconducting manganites approaching the metal-insulator transition. <b>2006</b> , 15, 498-507		3
683	The origin of the weak ferroelectric-like hysteresis effect in paraelectric Ba <sub>0.5</sub> Sr <sub>0.5</sub> TiO <sub>3</sub> thin films grown epitaxially on LaAlO <sub>3</sub> . <i>Journal of Physics Condensed Matter</i> , <b>2006</b> , 18, 4709-4718	1.8	17
682	High dielectric constant in charge-ordered Ca <sub>1.75</sub> Pr <sub>0.25</sub> MnO <sub>4</sub> . <b>2006</b> , 39, 1192-1196		8
681	Peculiar ferroelectric and dielectric properties of quasiperiodic PbZr <sub>0.4</sub> Ti <sub>0.6</sub> O <sub>3</sub> multilayers. <b>2006</b> , 8, 316-316		7
680	Effect of double-sided CaTiO <sub>3</sub> buffer layers on the electrical properties of CaCu <sub>3</sub> Ti <sub>4</sub> O <sub>12</sub> films on Pt/SiO <sub>2</sub> /Si substrates. <i>Journal of Applied Physics</i> , <b>2006</b> , 100, 104101	2.5	22
679	High-temperature memory in (Pb/La)(Zr/Ti)O <sub>3</sub> as intrinsic of the relaxor state rather than due to defect relaxation. <i>Physical Review B</i> , <b>2006</b> , 74,	3.3	3
678	Mechanism and scalability in resistive switching of metal-Pr <sub>0.7</sub> Ca <sub>0.3</sub> MnO <sub>3</sub> interface. <b>2006</b> , 89, 123502		28
677	Spin dynamics in the low-dimensional magnet TiOCl. <i>Physical Review B</i> , <b>2006</b> , 73,	3.3	28
676	Dielectric relaxation in pulsed laser ablated CaCu <sub>3</sub> Ti <sub>4</sub> O <sub>12</sub> thin film. <i>Journal of Applied Physics</i> , <b>2006</b> , 100, 034102	2.5	13
675	Doping dependence of polaron hopping energies in La <sub>1-x</sub> CaxMnO <sub>3</sub> (0 ≤ x ≤ 0.15). <i>Physical Review B</i> , <b>2006</b> , 74,	3.3	21
674	Dielectric Properties and Charge Transport in All-Organic Relaxorlike CuPc-P(VDF-TrFE-CFE) Composite and its Constituents. <b>2006</b> , 338, 107-116		15
673	High dielectric permittivity of Li and Ta codoped NiO ceramics. <b>2007</b> , 40, 863-868		45
672	Impedance of Sn <sub>24</sub> P <sub>19.3</sub> Br <sub>x</sub> I <sub>8-x</sub> semiconducting clathrates. <b>2007</b> , 33, 276-279		7

671	Giant dielectric behaviour of $\text{CaCu}_3\text{Ti}_4\text{O}_{12}$ subjected to post-sintering annealing and uniaxial stress. <i>Journal of Physics Condensed Matter</i> , <b>2007</b> , 19, 236208	1.8	30
670	Dielectric constant and ac conductivity of the layered cobalt oxide $\text{Bi}_2\text{Sr}_2\text{CoO}_6$ —A possible metal-dielectric composite made by self-organization of $\text{Co}^{2+}$ and $\text{Co}^{3+}$ ions. <i>Physical Review B</i> , <b>2007</b> , 76,	3.3	12
669	Evidence for the existence of a metal-insulator-semiconductor junction at the electrode interfaces of $\text{CaCu}_3\text{Ti}_4\text{O}_{12}$ thin film capacitors. <b>2007</b> , 91, 202903		60
668	Dielectric anomaly at TN in $\text{LaMnO}_3$ as a signature of coupling between spin and orbital degrees of freedom. <i>Physical Review B</i> , <b>2007</b> , 76,	3.3	14
667	Large enhancement in polarization response and energy density of poly(vinylidene fluoride-trifluoroethylene-chlorofluoroethylene) by interface effect in nanocomposites. <b>2007</b> , 91, 122909		70
666	Broadband dielectric spectroscopy on single-crystalline and ceramic $\text{CaCu}_3\text{Ti}_4\text{O}_{12}$ . <b>2007</b> , 91, 022910		125
665	Properties of highly (100) oriented $\text{Pb}(\text{Mg}_{1-x}\text{Nb}_x)\text{O}_3/\text{PbTiO}_3$ films on $\text{LaNiO}_3$ bottom electrodes. <b>2007</b> , 91, 232912		14
664	Grain-boundary and subgrain-boundary effects on the dielectric properties of $\text{CaCu}_3\text{Ti}_4\text{O}_{12}$ ceramics. <b>2007</b> , 40, 2899-2905		42
663	Dielectric Properties of $\text{CaCu}_3\text{Ti}_4\text{O}_{12}/\text{CaTiO}_3$ Multilayer Thin Films Synthesized by PLD Method. <b>2007</b> , 357, 191-195		
662	Dielectric Properties and Carrier Dynamics in $\text{Bi}_2\text{Sr}_2\text{YCu}_2\text{O}_8$ . <b>2007</b> , 76, 044711		4
661	$\text{CaCu}_3\text{Ti}_4\text{O}_{12}$ -type Colossal Dielectric Relaxation in Complex Perovskite $(\text{Ba}_{1-x}\text{La}_x)(\text{Ti}_{1-x}\text{Cr}_x)\text{O}_3$ . <b>2007</b> , 354, 106-114		1
660	Maxwell-Wagner relaxation in the $\text{CaMn}_7\text{O}_{12}$ perovskite. <b>2007</b> , 35, 379-386		8
659	Maxwell-Wagner polarization mechanism in potassium and titanium doped nickel oxide showing giant dielectric permittivity. <b>2007</b> , 40, 556-560		52
658	Effect of dc electric field on conductivity and giant permittivity of $\text{K}_x\text{Ti}_y\text{Ni}_{1-y}\text{O}$ . <b>2007</b> , 90, 242913		8
657	Synthesis of the Giant Dielectric Constant Material $\text{CaCu}_3\text{Ti}_4\text{O}_{12}$ by Wet-Chemistry Methods. <b>2007</b> , 19, 6020-6024		90
656	Origin of colossal dielectric response of $\text{CaCu}_3\text{Ti}_4\text{O}_{12}$ studied by using $\text{CaTiO}_3/\text{CaCu}_3\text{Ti}_4\text{O}_{12}/\text{CaTiO}_3$ multilayer thin films. <b>2007</b> , 90, 242904		14
655	New routes to multiferroics. <b>2007</b> , 17, 4931		149
654	Conducting grain boundaries in the high-dielectric-constant ceramic $\text{CaCu}_3\text{Ti}_4\text{O}_{12}$ . <i>Journal of Applied Physics</i> , <b>2007</b> , 101, 074101	2.5	12



653	Polaron relaxation related to localized charge carriers in CaCu <sub>3</sub> Ti <sub>4</sub> O <sub>12</sub> . <b>2007</b> , 90, 142905		86
652	Multiferroic nature of charge-ordered rare earth manganites. <i>Journal of Physics Condensed Matter</i> , <b>2007</b> , 19, 496217	1.8	34
651	Giant dielectric permittivity and magnetocapacitance in La <sub>0.875</sub> Sr <sub>0.125</sub> MnO <sub>3</sub> single crystals. <i>Physical Review B</i> , <b>2007</b> , 75,	3.3	30
650	Giant Dielectric Permittivity and Colossal Magnetocapacitance Effect in Complex Manganites with High Conductivity. <b>2007</b> , 348, 7-12		2
649	Synthesis and characterization of thin film multiferroic Ni <sub>3</sub> V <sub>2</sub> O <sub>8</sub> . <b>2007</b> , 87, 223-229		6
648	Dielectric and Electrical Properties of CaCu <sub>3</sub> Ti <sub>4</sub> O <sub>12</sub> Ceramics at High Temperatures. <b>2007</b> , 356, 85-89		4
647	Compression of CdCu <sub>3</sub> Ti <sub>4</sub> O <sub>12</sub> perovskite to 55 GPa. <b>2007</b> , 142, 376-379		1
646	Electrical heterogeneity in CaCu <sub>3</sub> Ti <sub>4</sub> O <sub>12</sub> ceramics fabricated by sol-gel method. <b>2007</b> , 142, 573-576		86
645	Effect of cation addition on dielectric properties of TbMnO <sub>3</sub> . <i>Physica B: Condensed Matter</i> , <b>2007</b> , 392, 147-150	2.8	6
644	Colossal magnetocapacitance and scale-invariant dielectric response in phase-separated manganites. <b>2007</b> , 3, 551-555		50
643	Evidence of Cu Deficiency: A Key Point for the Understanding of the Mystery of the Giant Dielectric Constant in CaCu <sub>3</sub> Ti <sub>4</sub> O <sub>12</sub> . <i>Journal of the American Ceramic Society</i> , <b>2007</b> , 90, 638-640	3.8	81
642	Electric and Dielectric Properties of Nb-Doped CaCu <sub>3</sub> Ti <sub>4</sub> O <sub>12</sub> Ceramics. <i>Journal of the American Ceramic Society</i> , <b>2007</b> , 90, 2118-2121	3.8	61
641	Effect of Al Doping on the Electric and Dielectric Properties of CaCu <sub>3</sub> Ti <sub>4</sub> O <sub>12</sub> . <i>Journal of the American Ceramic Society</i> , <b>2007</b> , 90, 070922001308001-???	3.8	7
640	Increase of the dielectric constant near a magnetic phase transition in La <sub>0.5</sub> Ca <sub>0.5</sub> MnO <sub>3</sub> . <b>2007</b> , 61, 2990-2992		9
639	Photoconductivity of the Pb <sub>0.75</sub> Sn <sub>0.25</sub> Te:In alloy in an alternating electric field. <b>2007</b> , 41, 663-665		2
638	Microwave synthesis and sintering characteristics of CaCu <sub>3</sub> Ti <sub>4</sub> O <sub>12</sub> . <b>2007</b> , 30, 567-570		24
637	Nanocrystalline CaCu <sub>3</sub> Ti <sub>4</sub> O <sub>12</sub> powders prepared by egg white solution route: synthesis, characterization and its giant dielectric properties. <i>Applied Physics A: Materials Science and Processing</i> , <b>2008</b> , 91, 87-95	2.6	37
636	Enhancement of Electrical Properties of Ferroelectric Polymers by Polyaniline Nanofibers with Controllable Conductivities. <b>2008</b> , 18, 1299-1306		129

635	Effect of laser fluence on the microstructure and dielectric properties of pulsed laser-deposited CaCu <sub>3</sub> Ti <sub>4</sub> O <sub>12</sub> thin films. <b>2008</b> , 310, 3470-3473		9
634	Nanoparticles of the giant dielectric material, CaCu <sub>3</sub> Ti <sub>4</sub> O <sub>12</sub> from a precursor route. <b>2008</b> , 69, 2594-2604		59
633	Colossal magnetocapacitive effect in differently synthesized and doped CdCr <sub>2</sub> S <sub>4</sub> . <i>Physica B: Condensed Matter</i> , <b>2008</b> , 403, 4224-4227	2.8	19
632	Dielectric properties of Sr <sub>3</sub> CuNb <sub>2</sub> O <sub>9</sub> perovskite ceramics. <b>2008</b> , 44, 1233-1239		7
631	Synthesis and giant dielectric behavior of CaCu <sub>3</sub> Ti <sub>4</sub> O <sub>12</sub> ceramics prepared by polymerized complex method. <i>Materials Chemistry and Physics</i> , <b>2008</b> , 109, 262-270	4.4	58
630	Sol-gel derived CaCu <sub>3</sub> Ti <sub>4</sub> O <sub>12</sub> ceramics: Synthesis, characterization and electrical properties. <i>Materials Research Bulletin</i> , <b>2008</b> , 43, 1800-1807	5.1	139
629	The effect of Cr <sub>2</sub> O <sub>3</sub> , Nb <sub>2</sub> O <sub>5</sub> and ZrO <sub>2</sub> doping on the dielectric properties of CaCu <sub>3</sub> Ti <sub>4</sub> O <sub>12</sub> . <b>2008</b> , 62, 633-636		91
628	Magnetization induced dielectric anomaly in multiferroic LaFeO <sub>3</sub> BbTiO <sub>3</sub> solid solution. <b>2008</b> , 93, 182908		40
627	Effects of interfacial polarization on the dielectric properties of BiFeO <sub>3</sub> thin film capacitors. <b>2008</b> , 92, 122903		81
626	Oxygen-vacancy-related dielectric relaxation in BiFeO <sub>3</sub> films grown by pulsed laser deposition. <b>2008</b> , 41, 215403		25
625	Colossal dielectric constants in single-crystalline and ceramic CaCu <sub>3</sub> Ti <sub>4</sub> O <sub>12</sub> investigated by broadband dielectric spectroscopy. <i>Journal of Applied Physics</i> , <b>2008</b> , 103, 084107	2.5	165
624	Dielectric responses and multirelaxation behaviors of pure and doped CaCu <sub>3</sub> Ti <sub>4</sub> O <sub>12</sub> ceramics. <i>Journal of Applied Physics</i> , <b>2008</b> , 104, 064110	2.5	31
623	Anomalous current-voltage behavior of CaCu <sub>3</sub> Ti <sub>4</sub> O <sub>12</sub> ceramics. <b>2008</b> , 93, 182912		17
622	Synthesis, structural, magnetic and transport properties of layered perovskite-related titanates, niobates and tantalates of the type AnBnO <sub>3n+2</sub> , A <sub>2</sub> Ak <sub>2</sub> BkO <sub>3k+1</sub> and AmBm <sub>2</sub> O <sub>3m</sub> . <b>2008</b> , 36, 253-387		121
621	Optical spectroscopy in CoO: Phononic, electric, and magnetic excitation spectrum within the charge-transfer gap. <i>Physical Review B</i> , <b>2008</b> , 78,	3.3	46
620	Magneto-transport and magneto-dielectric effects in Bi-based perovskite manganites. <b>2008</b> , 18, 4280		12
619	Dc-bias-field-induced dielectric relaxation and ac conduction in CaCu <sub>3</sub> Ti <sub>4</sub> O <sub>12</sub> ceramics. <b>2008</b> , 88, 537-545		38
618	Localized electrical characterization of the giant permittivity effect in CaCu <sub>3</sub> Ti <sub>4</sub> O <sub>12</sub> ceramics. <b>2008</b> , 92, 182907		44

617	Giant dielectric anisotropy and relaxor ferroelectricity induced by proton transfers in NH+...N-bonded supramolecular aggregates. <b>2008</b> , 112, 6779-85		57
616	High dielectric permittivity observed in Na and Al doped NiO. <b>2008</b> , 41, 155416		12
615	RAMAN AND DIELECTRIC SPECTRA OF CaCu3Ti3.9O12 CERAMICS. <b>2008</b> , 97, 143-150		14
614	Preparation and Properties of CaCu3Ti4O12 Thick Film by Aerosol Deposition Method. <b>2008</b> , 368-372, 126-128		
613	Physical origin of colossal dielectric constant in CaCu3Ti4O12 thin film by Pulsed Laser Deposition. <b>2008</b> , 1073, 1		
612	First-principles electronic structure and lattice dynamics of the giant dielectric compound Na0.5Bi0.5Cu3Ti4O12. <i>Journal of Physics Condensed Matter</i> , <b>2008</b> , 20, 175220	1.8	3
611	A low-temperature specific heat study of giant dielectric constant materials. <i>Journal of Physics Condensed Matter</i> , <b>2008</b> , 20, 285214	1.8	3
610	Preparation of Mg and Ti Co-Doped NiO-Based Ceramic and its High Dielectric Properties. <b>2008</b> , 368-372, 37-39		
609	Dielectric Properties of MgAl2O4 Transparent Nano-Ceramic. <b>2008</b> , 368-372, 412-413		0
608	Anomalous thermal hysteresis in dielectric permittivity of CaCu3Ti4O12. <b>2008</b> , 92, 132903		22
607	Enhanced dielectric responses in Mg-doped CaCu3Ti4O12. <i>Journal of Applied Physics</i> , <b>2008</b> , 104, 074107	2.5	57
606	Structural and optical studies of high dielectric constant (Na(0.5)A(0.5))Cu(3)Ti(4)O(12) (A = La and Bi). <i>Journal of Physics Condensed Matter</i> , <b>2008</b> , 20, 275238	1.8	5
605	Dielectric Properties of the Charge Ordered Oxyborate Fe <sub>2</sub> OBO <sub>3</sub> . <b>2008</b> , 44, 2989-2992		4
604	A multiferroic ceramic with perovskite structure: (La0.5Bi0.5)(Mn0.5Fe0.5)O3.09. <b>2008</b> , 93, 052906		33
603	Magnetocapacitance in nonmagnetic composite media. <b>2008</b> , 101, 166602		52
602	Interfacial contribution to the dielectric response in semiconducting LaBiMn4BCo2BO6. <b>2008</b> , 92, 212905		23
601	Broadband dielectric response of CaCu3Ti4O12: From dc to the electronic transition regime. <i>Physical Review B</i> , <b>2008</b> , 77,	3-3	47
600	. <b>2008</b> ,		1

599	Interfacial resistive oxide switch induced by reversible modification of defect structures. <i>Physical Review B</i> , <b>2009</b> , 80,	3.3	4
598	Perovskite CaCu <sub>3</sub> Ti <sub>4</sub> O <sub>12</sub> thin films for capacitive applications: From the growth to the nanoscopic imaging of the permittivity. <i>Journal of Applied Physics</i> , <b>2009</b> , 105, 061634	2.5	24
597	DIELECTRIC PROPERTIES OF NEW BiLi <sub>0.5</sub> Sb <sub>0.5</sub> O <sub>3</sub> CERAMICS. <b>2009</b> , 109, 61-69		3
596	Defects in codoped NiO with gigantic dielectric response. <i>Physical Review B</i> , <b>2009</b> , 79,	3.3	10
595	Manifestation of the electrode-contact effect on the dielectric response and impedance spectra of CaSiO <sub>3</sub> -doped CaCu <sub>3</sub> Ti <sub>4</sub> O <sub>12</sub> . <i>Journal of Applied Physics</i> , <b>2009</b> , 106, 054106	2.5	14
594	Investigation on the decomposable process and the secondary liquid phase effect on the dielectric properties of CaCu <sub>3</sub> Ti <sub>4</sub> O <sub>12</sub> ceramics. <b>2009</b> , 42, 175401		19
593	Grain size effect on the permittivity of La <sub>1.5</sub> Sr <sub>0.5</sub> NiO <sub>4</sub> nanoparticles. <b>2009</b> , 187, 012085		5
592	Temperature dependence of electron spin resonance in CaCu <sub>3</sub> Ti <sub>4</sub> O <sub>12</sub> substituted with transition metal elements. <b>2009</b> , 11, 875-880		13
591	Nanocomposites of Ferroelectric Polymers with TiO <sub>2</sub> Nanoparticles Exhibiting Significantly Enhanced Electrical Energy Density. <b>2009</b> , 21, 217-221		423
590	Relationship among the phase equilibria, microstructures, and dielectric properties of CaCu <sub>3</sub> Ti <sub>4</sub> O <sub>12</sub> ceramics via different sintering time. <b>2009</b> , 44, 4117-4123		20
589	Effect of Rapid Thermal Annealing on Sputtered CaCu <sub>3</sub> Ti <sub>4</sub> O <sub>12</sub> Thin Films. <b>2009</b> , 38, 453-459		11
588	Nanocrystalline CaCu <sub>3</sub> Ti <sub>4</sub> O <sub>12</sub> powder by PVA sol-gel route: synthesis, characterization and its giant dielectric constant. <i>Applied Physics A: Materials Science and Processing</i> , <b>2009</b> , 96, 595-602	2.6	13
587	Dielectric relaxation and giant dielectric constant of Nb-doped CaCu <sub>3</sub> Ti <sub>4</sub> O <sub>12</sub> ceramics under dc bias voltage. <i>Physica Status Solidi (A) Applications and Materials Science</i> , <b>2009</b> , 206, 562-566	1.6	16
586	Circuit simulation for the dielectric responses of the composites of copper phthalocyanine oligomers and sulfonated polyurethanes by separating the structural elements. <b>2009</b> , 47, 1146-1155		8
585	Giant Dielectric Response with an Electric Field in Charge-Ordered La <sub>1-x</sub> CaxMnO <sub>3</sub> Compounds. <i>Journal of the American Ceramic Society</i> , <b>2009</b> , 92, 1366-1369	3.8	8
584	Pseudo-relaxor behaviour induced by Maxwell-Wagner relaxation. <b>2009</b> , 149, 2017-2020		37
583	Effect of thickness on the dielectric property and nonlinear current-voltage behavior of CaCu <sub>3</sub> Ti <sub>4</sub> O <sub>12</sub> thin films. <b>2009</b> , 373, 2389-2392		15
582	Electrical and dielectric behaviors and their origins in the three-dimensional polyvinyl alcohol/MWCNT composites with low percolation threshold. <b>2009</b> , 47, 1311-1320		165

581	Correlations of structural, magnetic, and dielectric properties of undoped and doped CaCu <sub>3</sub> Ti <sub>4</sub> O <sub>12</sub> . <b>2009</b> , 72, 173-182		53
580	Colossal dielectric constants in transition-metal oxides. <b>2009</b> , 180, 61-89		304
579	Low-frequency dynamic response of the bismuth strontium ferrite (Bi,Sr)FeO <sub>3</sub> . <b>2009</b> , 51, 498-502		4
578	Effects of Interfacial Polarization on Voltage Tunability of Pb(Fe 1/2 Nb 1/2 ) 1x Ti x O 3 Single Crystals. <b>2009</b> , 26, 107701		2
577	Electrical properties and microstructural characteristics of nonstoichiometric CaCu <sub>3</sub> xTi <sub>4</sub> O <sub>12</sub> ceramics. <i>Journal of Alloys and Compounds</i> , <b>2009</b> , 469, 529-534	5-7	65
576	Effects of cation stoichiometry on the dielectric properties of CaCu <sub>3</sub> Ti <sub>4</sub> O <sub>12</sub> . <i>Journal of Alloys and Compounds</i> , <b>2009</b> , 473, 433-436	5-7	50
575	Dielectric properties of the Ca <sub>1-x</sub> La <sub>x</sub> Cu <sub>3</sub> Ti <sub>4</sub> CoxO <sub>12</sub> system (x=0.10, 0.20 and 0.30) synthesized by semi-wet route. <i>Journal of Alloys and Compounds</i> , <b>2009</b> , 478, 771-776	5-7	27
574	Influence of the cationic ordering in the dielectric properties of the La <sub>2</sub> MnCoO <sub>6</sub> perovskite. <i>Journal of Alloys and Compounds</i> , <b>2009</b> , 485, 82-87	5-7	37
573	Giant permittivity and MaxwellWagner relaxation in Yb : CaTiO <sub>3</sub> ceramics. <b>2009</b> , 42, 175407		34
572	Polymer Composite and Nanocomposite Dielectric Materials for Pulse Power Energy Storage. <b>2009</b> , 2, 1697-1733		564
571	Relaxations as key to the magnetocapacitive effects in the perovskite manganites. <b>2009</b> , 102, 207208		61
570	Dielectric dispersion of BiFeO <sub>3</sub> thin film over a broad frequency range (100 Hz-10 GHz). <b>2009</b> , 94, 022907		42
569	Dielectric dispersion of BaxSr1-xTiO <sub>3</sub> thin film with parallel-plate and coplanar interdigital electrodes. <b>2009</b> , 42, 065411		3
568	Colossal dielectric behavior of semiconducting Sr <sub>2</sub> TiMnO <sub>6</sub> ceramics. <i>Journal of Applied Physics</i> , <b>2009</b> , 105, 034113	2.5	50
567	Colossal dielectric constant up to gigahertz at room temperature. <b>2009</b> , 94, 122903		153
566	Electrical characterization of resistive memory in metal-Pr <sub>0.7</sub> Ca <sub>0.3</sub> MnO <sub>3</sub> interface: A future non-volatile memory device. <b>2009</b> ,		
565	Detection of heterogeneities in single-crystal CaCu <sub>3</sub> Ti <sub>4</sub> O <sub>12</sub> using conductive atomic force microscopy. <b>2010</b> , 8, 012018		2
564	Ion sweeping in conducting dielectric materials. <b>2010</b> , 75, 209-216		13

563	Structure, charge ordering and physical properties of Yb <sub>2</sub> Fe <sub>3</sub> O <sub>7</sub> . <b>2010</b> , 75, 231-236		7
562	On the room temperature multiferroic BiFeO <sub>3</sub> : magnetic, dielectric and thermal properties. <b>2010</b> , 75, 451-460		115
561	Slicing the perovskite structure with crystallographic shear planes: the A(n)B(n)O(3n-2) homologous series. <b>2010</b> , 49, 9508-16		22
560	Influence of the processing rates and sintering temperatures on the dielectric properties of CaCu <sub>3</sub> Ti <sub>4</sub> O <sub>12</sub> ceramics. <b>2010</b> , 24, 231-236		23
559	Influence of high levels of Nb and Ti doping on the dielectric properties of CaCu <sub>3</sub> Ti <sub>4</sub> O <sub>12</sub> type of compounds. <i>Materials Chemistry and Physics</i> , <b>2010</b> , 120, 576-581	4.4	12
558	Trap state capture and reemission relaxation in ceramic La <sub>1-x</sub> CaxMnO <sub>3</sub> with Ca-content x=0.51. <i>Physica B: Condensed Matter</i> , <b>2010</b> , 405, 999-1003	2.8	5
557	Humidity sensitive properties of pure and Mg-doped CaCu <sub>3</sub> Ti <sub>4</sub> O <sub>12</sub> . <b>2010</b> , 147, 447-452		71
556	Colossal dielectric constants: A common phenomenon in CaCu <sub>3</sub> Ti <sub>4</sub> O <sub>12</sub> related materials. <b>2010</b> , 150, 857-860		53
555	Dielectric properties of Poly(vinylidene fluoride)/CaCu <sub>3</sub> Ti <sub>4</sub> O <sub>12</sub> composites. <b>2010</b> , 70, 539-545		229
554	The Synthesis of Pure-Phase Bismuth Ferrite in the BiFeO <sub>3</sub> System Under Hydrothermal Conditions without a Mineralizer. <i>Journal of the American Ceramic Society</i> , <b>2010</b> , 93, 3173-3179	3.8	22
553	Magnetodielectric Effect and Tunable Dielectric Properties of LaMn <sub>1-x</sub> FexO <sub>3</sub> . <i>Journal of the American Ceramic Society</i> , <b>2010</b> , 93, 3814-3818	3.8	10
552	Dielectric permittivity and electrical conductivity of polycrystalline materials. <b>2010</b> , 46, 1365-1368		6
551	Out-of-Plane Dielectric Behavior of Insulating Bi <sub>2</sub> Sr <sub>2</sub> RECu <sub>2</sub> O <sub>8</sub> (RE= Dy, Y, and Er). <b>2010</b> , 79, 054709		4
550	Temperature- and Frequency-Dependent Dielectric Properties of La <sub>1.5</sub> Sr <sub>0.5</sub> NiO <sub>4</sub> . <b>2010</b> , 27, 087701		1
549	Giant low frequency dielectric tunability in high-k Ba(Fe <sub>1/2</sub> Nb <sub>1/2</sub> )O <sub>3</sub> ceramics at room temperature. <i>Journal of Applied Physics</i> , <b>2010</b> , 108, 064104	2.5	21
548	Colossal dielectric constant and relaxation behaviors in Pr:SrTiO <sub>3</sub> ceramics. <i>Journal of Applied Physics</i> , <b>2010</b> , 107, 094108	2.5	24
547	Intrinsic and extrinsic relaxation of CaCu <sub>3</sub> Ti <sub>4</sub> O <sub>12</sub> ceramics: Effect of sintering. <i>Journal of Applied Physics</i> , <b>2010</b> , 108, 104104	2.5	61
546	Reorientable dipolar CuCa antisite and anomalous screening in CaCu <sub>3</sub> Ti <sub>4</sub> O <sub>12</sub> . <i>Physical Review B</i> , <b>2010</b> , 81,	3.3	10

545	Magnetodielectric response in the charge ordered oxyborate Fe <sub>2</sub> OBO <sub>3</sub> . <i>Journal of Applied Physics</i> , <b>2010</b> , 108, 074115	2.5	4
544	Colossal dielectric constants in La <sub>15/8</sub> Sr <sub>1/8</sub> NiO <sub>4</sub> . <b>2010</b> , 8, 012014		4
543	Annealing effects on electrical properties and defects of CaCu <sub>3</sub> Ti <sub>4</sub> O <sub>12</sub> thin films deposited by pulsed laser deposition. <i>Physical Review B</i> , <b>2010</b> , 81,	3.3	21
542	High-temperature dielectric response of (1-x)Pb(Mg <sub>1/3</sub> Nb <sub>2/3</sub> )O <sub>3</sub> -xPbTiO <sub>3</sub> : Does Burns temperature exist in ferroelectric relaxors?. <i>Journal of Applied Physics</i> , <b>2010</b> , 107, 084104	2.5	25
541	Non-symmetrical electric response in CaCu <sub>3</sub> Ti <sub>4</sub> O <sub>12</sub> and La <sub>0.05</sub> Ba <sub>0.95</sub> TiO <sub>3</sub> -PZT materials. <b>2010</b> , 43, 385401		4
540	The effects of grain boundary response and electrode contact response on the dielectric properties of CaCu <sub>3</sub> Ti <sub>4</sub> O <sub>12</sub> . <b>2010</b> , 43, 295405		10
539	Glassiness in charge dynamics of half-doped manganite: A study on oxygen-deficient charge-ordered R <sub>0.5</sub> Ca <sub>0.5</sub> MnO <sub>3</sub> (R = Pr, Nd and Sm). <b>2010</b> , 92, 57009		8
538	Bulk dielectric and magnetic properties of PFW-PZT ceramics: absence of magnetically switched-off polarization. <i>Journal of Physics Condensed Matter</i> , <b>2010</b> , 22, 445902	1.8	11
537	Dielectric Grain-Size Effect in High-Permittivity Ceramics. <b>2010</b> , 400, 117-134		57
536	Characterization of nickel doped CCTO: CaCu <sub>2.9</sub> Ni <sub>0.1</sub> Ti <sub>4</sub> O <sub>12</sub> and CaCu <sub>3</sub> Ti <sub>3.9</sub> Ni <sub>0.1</sub> O <sub>12</sub> synthesized by semi-wet route. <i>Journal of Alloys and Compounds</i> , <b>2010</b> , 491, 507-512	5.7	57
535	BiMnFe <sub>2</sub> O <sub>6</sub> , a polysynthetically twinned hcp MO structure. <b>2010</b> , 1, 751		13
534	Phase coexistence and multiple dielectric relaxations in the single layered manganite Nd <sub>0.22</sub> Sr <sub>1.78</sub> MnO <sub>4</sub> . <i>Journal of Applied Physics</i> , <b>2010</b> , 107, 014108	2.5	8
533	Dielectric, magnetic, and lattice dynamics properties of Y-type hexaferrite Ba <sub>0.5</sub> Sr <sub>1.5</sub> Zn <sub>2</sub> Fe <sub>12</sub> O <sub>22</sub> : Comparison of ceramics and single crystals. <i>Journal of Applied Physics</i> , <b>2010</b> , 107, 104109	2.5	31
532	Ferroelectric Polymer Based Nanocomposites for Electrical Energy Storage. <i>ACS Symposium Series</i> , <b>2010</b> , 37-52	0.4	5
531	Morphology-controllable graphene/TiO <sub>2</sub> nanorod hybrid nanostructures for polymer composites with high dielectric performance. <b>2011</b> , 21, 17729		114
530	Dielectric Properties of CaCu <sub>3</sub> Ti <sub>4</sub> O <sub>12</sub> Ceramic Thin Films. <b>2011</b> , 419, 14-19		1
529	Preparation and dielectric properties of CaCu <sub>3</sub> Ti <sub>4</sub> O <sub>12</sub> -(NaBi) <sub>0.5</sub> Cu <sub>3</sub> Ti <sub>4</sub> O <sub>12</sub> composites. <b>2011</b> ,		
528	Magnetodielectric response in 0.36BiScO <sub>3</sub> -0.64PbTiO <sub>3</sub> /La <sub>0.7</sub> Sr <sub>0.3</sub> MnO <sub>3</sub> thin films and the corresponding model modifications. <i>Journal of Applied Physics</i> , <b>2011</b> , 110, 046103	2.5	11



527	High temperature dielectric properties of YMnO <sub>3</sub> ceramics. <i>Journal of Applied Physics</i> , <b>2011</b> , 110, 064116-5	2.5	30
526	Non-linear dielectric properties of BiFeO <sub>3</sub> ceramics. <b>2011</b> , 99, 172904		14
525	Intrinsic and extrinsic dielectric responses of CaCu <sub>3</sub> Ti <sub>4</sub> O <sub>12</sub> thin films. <i>Journal of Applied Physics</i> , <b>2011</b> , 110, 074102	2.5	7
524	High-temperature dielectric response of ferroelectric relaxors. <b>2011</b> , 58, 2270-5		1
523	Voltage dependent capacitances in CaCu <sub>3</sub> Ti <sub>4</sub> O <sub>12</sub> . <i>Journal of Applied Physics</i> , <b>2011</b> , 109, 084113	2.5	15
522	Magnetic field modulated dielectric relaxation behavior of Pt/BiScO <sub>3</sub> -PbTiO <sub>3</sub> /La <sub>0.7</sub> Sr <sub>0.3</sub> MnO <sub>3</sub> heterostructure in metal-insulator transition region: An equivalent-circuit method. <i>Journal of Applied Physics</i> , <b>2011</b> , 110, 114118	2.5	3
521	Spin-reorientation, ferroelectricity, and magnetodielectric effect in YFe(1-x)Mn(x)O <sub>3</sub> (0.1 <math>x</math> 0.40). <b>2011</b> , 107, 137202		113
520	Tuning A-site ionic size in R(0.5)Ca(0.5)MnO <sub>3</sub> (R = Pr, Nd and Sm): robust modulation in dc and ac transport behavior. <i>Journal of Physics Condensed Matter</i> , <b>2011</b> , 23, 495902	1.8	10
519	Origin of the colossal dielectric permittivity and magnetocapacitance in LuFe <sub>2</sub> O <sub>4</sub> . <i>Journal of Applied Physics</i> , <b>2011</b> , 109, 074109	2.5	45
518	Thin film colossal dielectric constant oxide La <sub>2-x</sub> Sr <sub>x</sub> NiO <sub>4</sub> : Synthesis, dielectric relaxation measurements, and electrode effects. <i>Journal of Applied Physics</i> , <b>2011</b> , 109, 014106	2.5	19
517	Broadband dielectric spectroscopy on human blood. <b>2011</b> , 1810, 727-40		100
516	An aqueous-solution based low-temperature pathway to synthesize giant dielectric CaCu <sub>3</sub> Ti <sub>4</sub> O <sub>12</sub> highly porous ceramic matrix and submicron sized powder. <i>Journal of Alloys and Compounds</i> , <b>2011</b> , 509, 4381-4385	5.7	19
515	Improved dielectric and non-ohmic properties of Ca <sub>2</sub> Cu <sub>2</sub> Ti <sub>4</sub> O <sub>12</sub> ceramics prepared by a polymer pyrolysis method. <i>Journal of Alloys and Compounds</i> , <b>2011</b> , 509, 7416-7420	5.7	35
514	Slow Trap Charge Repositioning Processes and the Polarization of CaCu <sub>3</sub> Ti <sub>4</sub> O <sub>12</sub> . <i>Journal of the American Ceramic Society</i> , <b>2011</b> , 94, 2512-2517	3.8	12
513	Dielectric and Varistor Behavior of CaCu <sub>3</sub> Ti <sub>4</sub> O <sub>12</sub> /MgTiO <sub>3</sub> Composite Ceramics. <i>Journal of the American Ceramic Society</i> , <b>2011</b> , 94, 1966-1969	3.8	38
512	Influence of Preparation Conditions on Distinctive Contributions to Dielectric Behavior of CaCu <sub>3</sub> Ti <sub>4</sub> O <sub>12</sub> Thin Films. <i>Journal of the American Ceramic Society</i> , <b>2011</b> , 94, 3900-3906	3.8	10
511	Schottky-type grain boundaries in CCTO ceramics. <b>2011</b> , 151, 1377-1381		68
510	Colossal dielectric constant and a microfarad tunable capacitance in platinum thin film-antimony doped barium strontium titanate Schottky barrier diodes. <i>Thin Solid Films</i> , <b>2011</b> , 520, 633-640	2.2	4



509	Ferroelectric behavior of titanium oxygen octahedral amorphous CaCu <sub>3</sub> Ti <sub>4</sub> O <sub>12</sub> thin film. <i>Materials Chemistry and Physics</i> , <b>2011</b> , 129, 394-397	4.4	3
508	Antiferroelectric (Pb,Bi) <sub>1-x</sub> Fe <sub>1+x</sub> O <sub>3</sub> Perovskites Modulated by Crystallographic Shear Planes. <b>2011</b> , 23, 255-265		30
507	Skin layer of BiFeO <sub>3</sub> single crystals. <b>2011</b> , 106, 236101		72
506	Electrode polarization effects in broadband dielectric spectroscopy. <b>2011</b> , 83, 157-165		93
505	Dielectric properties of CaCu <sub>3</sub> Ti <sub>4</sub> O <sub>12</sub> prepared by sol-gel self combustion technique. <i>Journal of Materials Science: Materials in Electronics</i> , <b>2011</b> , 22, 579-582	2.1	21
504	Temperature-dependent ac conductivity and dielectric response of vanadium doped CaCu <sub>3</sub> Ti <sub>4</sub> O <sub>12</sub> ceramic. <i>Applied Physics A: Materials Science and Processing</i> , <b>2011</b> , 104, 1105-1111	2.6	11
503	Origin of colossal dielectric response in LaFeO <sub>3</sub> . <b>2011</b> , 59, 1338-1345		167
502	Greatly enhanced energy density and patterned films induced by photo cross-linking of poly(vinylidene fluoride-chlorotrifluoroethylene). <b>2011</b> , 32, 94-9		51
501	Impedance study of giant dielectric permittivity in BaTi <sub>0.4</sub> (Fe <sub>0.5</sub> Nb <sub>0.5</sub> ) <sub>0.6</sub> O <sub>3</sub> ceramic. <i>Physica B: Condensed Matter</i> , <b>2011</b> , 406, 3470-3474	2.8	18
500	Effects of Pr Substitution on Electrical Properties of Bi(Fe <sub>0.95</sub> Mn <sub>0.05</sub> )O <sub>3</sub> Thin Films. <i>Japanese Journal of Applied Physics</i> , <b>2011</b> , 50, 01BF07	1.4	1
499	Anisotropic Colossal Dielectric Response of 0.93Pb(Fe <sub>1/2</sub> Nb <sub>1/2</sub> )O <sub>3</sub> ·0.07PbTiO <sub>3</sub> Single Crystals along [100] and [111] Directions. <i>Japanese Journal of Applied Physics</i> , <b>2011</b> , 50, 101502	1.4	1
498	Electrodynamics response of the charge ordering phase: Dielectric and optical studies of (BEDT-TTF) <sub>2</sub> I <sub>3</sub> . <i>Physical Review B</i> , <b>2011</b> , 83,	3.3	62
497	Relaxor ferroelectricity and the freezing of short-range polar order in magnetite. <i>Physical Review B</i> , <b>2011</b> , 83,	3.3	40
496	. <b>2011</b> ,		1
495	Magnetic and dielectric properties of Ba <sub>12</sub> Fe <sub>28</sub> Ti <sub>15</sub> O <sub>84</sub> layered ferrite ceramics. <b>2011</b> , 44, 435002		7
494	Reassessment of the impedance spectra and dielectric responses of undoped and CaSiO <sub>3</sub> -doped CaCu <sub>3</sub> Ti <sub>4</sub> O <sub>12</sub> . <i>Journal of Applied Physics</i> , <b>2011</b> , 109, 014102	2.5	14
493	Correlation between the trap state spectra and dielectric behavior of CaCu <sub>3</sub> Ti <sub>4</sub> O <sub>12</sub> . <b>2011</b> , 26, 36-44		22
492	Huge Dielectric Properties of CdCu <sub>3</sub> Ti <sub>4</sub> O <sub>12</sub> with CCTO Structure. <b>2011</b> , 415, 94-100		12

491	Correlation between the trap state spectra and dielectric behavior of CaCu <sub>3</sub> Ti <sub>4</sub> O <sub>12</sub> . <b>2011</b> , 26, 395-406		16
490	Charge Transport in Charge-Ordered States of Two-Dimensional Organic Conductors, $\beta$ (BEDT-TTF) <sub>2</sub> I <sub>3</sub> and $\beta$ (BEDT-TTF) <sub>2</sub> Br <sub>2</sub> . <b>2012</b> , 81, 044703		13
489	Absence of ferroelectricity in BiMnO <sub>3</sub> ceramics. <i>Journal of Applied Physics</i> , <b>2012</b> , 112, 074112	2.5	31
488	Doped polymer electrodes for high performance ferroelectric capacitors on plastic substrates. <b>2012</b> , 101, 143303		17
487	Annealing induced colossal magnetocapacitance and colossal magnetoresistance in In-doped CdCr <sub>2</sub> S <sub>4</sub> . <i>Journal of Applied Physics</i> , <b>2012</b> , 112, 123912	2.5	6
486	Dielectric and magnetic permittivities of three new ceramic tungstates MPr <sub>2</sub> W <sub>2</sub> O <sub>10</sub> (M = Cd, Co, Mn). <b>2012</b> , 92, 4167-4181		22
485	High-field magnetization and magnetoresistance of the A-site ordered perovskite oxide CaCu <sub>3</sub> Ti <sub>4</sub> Ru <sub>x</sub> O <sub>12</sub> (0 ≤ x ≤ 4). <i>Physical Review B</i> , <b>2012</b> , 85,	3.3	4
484	DIELECTRIC RELAXATION IN RELAXOR FERROELECTRICS. <b>2012</b> , 02, 1241010		212
483	Influence of Zn doping on microstructures and dielectric properties in CaCu <sub>3</sub> Ti <sub>4</sub> O <sub>12</sub> ceramic synthesised by semiwet route. <b>2012</b> , 111, 374-380		21
482	Photocarrier collection from depletion layer of LaMnO <sub>3</sub> . <i>Journal of Applied Physics</i> , <b>2012</b> , 111, 016107	2.5	8
481	Phonons in lanthanum manganite: Inelastic neutron scattering and density functional theory studies. <i>Physical Review B</i> , <b>2012</b> , 86,	3.3	2
480	Absence of polar order in LuFe <sub>2</sub> O <sub>4</sub> . <b>2012</b> , 85, 1		46
479	Giant Dielectric Constant Materials and Their Applications. <b>2012</b> , 123-146		1
478	Modeling of thickness effect and polarization saturation in electrostrictive polymers. <b>2012</b> , 171-172, 739-746		3
477	Dielectric properties of (Bi <sub>0.9</sub> La <sub>0.1</sub> ) <sub>2</sub> NiMnO <sub>6</sub> thin films: Determining the intrinsic electric and magnetoelectric response. <i>Physical Review B</i> , <b>2012</b> , 86,	3.3	23
476	Dielectric response of epitaxially strained CoFe <sub>2</sub> O <sub>4</sub> spinel thin films. <i>Physical Review B</i> , <b>2012</b> , 86,	3.3	22
475	Dielectric properties of CaCu <sub>3</sub> Ti <sub>4</sub> O <sub>12</sub> thick films. <b>2012</b> ,		
474	Complex Conductivity Using Wideband Spectroscopy for Yttria/Ytterbia-Stabilized Zirconia Ceramics. <i>Japanese Journal of Applied Physics</i> , <b>2012</b> , 51, 011102	1.4	2

473	Dielectric studies on the heterogeneity and interfacial property of composites made of polyacene quinone radical polymers and sulfonated polyurethanes. <b>2012</b> , 116, 2024-31		14
472	Apparent Colossal Dielectric Constants in Nanoporous Metal Organic Frameworks. <b>2012</b> , 116, 13026-13032		26
471	Electrical and Dielectric Properties of Exfoliated Graphite/Polyimide Composite Films with Low Percolation Threshold. <b>2012</b> , 41, 2439-2446		13
470	Stress and defect induced enhanced low field magnetoresistance and dielectric constant in La <sub>0.7</sub> Sr <sub>0.3</sub> MnO <sub>3</sub> thin films. <i>Journal of Alloys and Compounds</i> , <b>2012</b> , 512, 332-339	5.7	27
469	Dielectric signature of charge order in lanthanum nickelates. <b>2012</b> , 85, 1		12
468	Wtite: electric, thermodynamic and optical properties of FeO. <b>2012</b> , 85, 1		28
467	Dielectric dynamics of epitaxial BiFeO <sub>3</sub> thin films. <b>2012</b> , 2, 022133		4
466	Small polaronic hole hopping mechanism and Maxwell-Wagner relaxation in NdFeO <sub>3</sub> . <i>Journal of Applied Physics</i> , <b>2012</b> , 112, 074105	2.5	78
465	Between Molecule and Solid. <b>2012</b> , 379-394		
464	Dielectric properties of charge-ordered LuFe(2)O(4) revisited: the apparent influence of contacts. <b>2012</b> , 109, 016405		69
463	High Dielectric Constant and Relaxation Mechanism of Water with Hydrated Copper(II) Ions in a Cucurbit[8]uril-Based Supramolecular Architecture. <b>2012</b> , 116, 14199-14204		7
462	Giant dielectric response of Haldane gap compound Y <sub>2</sub> BaNiO <sub>5</sub> . <i>Journal of Applied Physics</i> , <b>2012</b> , 111, 064111	2.5	8
461	Dynamics of multiple phases in a colossal-magnetoresistive manganite as revealed by dielectric spectroscopy. <b>2012</b> , 3, 944		14
460	Magnetocapacitance effect in nonmultiferroic YFeO <sub>3</sub> single crystal. <i>Journal of Applied Physics</i> , <b>2012</b> , 111, 034103	2.5	46
459	High-performance non-volatile organic ferroelectric memory on banknotes. <b>2012</b> , 24, 2165-70		129
458	Low-temperature ferroelectric phase and magnetoelectric coupling in underdoped La <sub>2</sub> CuO <sub>4+x</sub> . <i>Physical Review B</i> , <b>2012</b> , 85,	3.3	14
457	Voltage-Current Nonlinearity of CaCu <sub>3</sub> Ti <sub>4</sub> O <sub>12</sub> Ceramics. <i>Journal of the American Ceramic Society</i> , <b>2012</b> , 95, 476-479	3.8	42
456	Effect of cesium and cerium substitution on the dielectric properties of CaCu <sub>3</sub> Ti <sub>4</sub> O <sub>12</sub> ceramics. <i>Ceramics International</i> , <b>2012</b> , 38, S65-S68	5.1	6

455	Effect of the MgO substitution for CuO on the properties of CaCu <sub>3</sub> Ti <sub>4</sub> O <sub>12</sub> ceramics. <i>Ceramics International</i> , <b>2012</b> , 38, 3459-3464	5.1	20
454	Bulk single crystal growth and characterization of l-leucine A nonlinear optical material. <i>Materials Chemistry and Physics</i> , <b>2012</b> , 133, 1055-1059	4.4	20
453	Comparative studies of ferroelectric behavior in rutile type FeTiTaO <sub>6</sub> and AlTiTaO <sub>6</sub> . <i>Materials Research Bulletin</i> , <b>2012</b> , 47, 184-187	5.1	10
452	Broadband spectroscopy of the complex conductivity of polycrystalline yttria-stabilized zirconia. <b>2012</b> , 177, 69-73		7
451	Impedance and electric modulus approaches to investigate four origins of giant dielectric constant in CaCu <sub>3</sub> Ti <sub>4</sub> O <sub>12</sub> ceramics. <b>2012</b> , 14, 330-334		21
450	Influence of Lu <sub>2</sub> O <sub>3</sub> on electrical and microstructural properties of CaCu <sub>3</sub> Ti <sub>4</sub> O <sub>12</sub> ceramics. <i>Physica B: Condensed Matter</i> , <b>2012</b> , 407, 2385-2389	2.8	24
449	Fundamentals, processes and applications of high-permittivity polymer matrix composites. <b>2012</b> , 57, 660-723		1185
448	Effect of calcium stoichiometry on the dielectric response of CaCu <sub>3</sub> Ti <sub>4</sub> O <sub>12</sub> ceramics. <b>2012</b> , 32, 1681-1690		30
447	Improvement in dielectric and mechanical performance of CaCu <sub>3.1</sub> Ti <sub>4</sub> O <sub>12.1</sub> by addition of Al <sub>2</sub> O <sub>3</sub> nanoparticles. <b>2012</b> , 7, 68		18
446	Dielectric properties of Erbium doped CaCu <sub>3</sub> Ti <sub>4</sub> O <sub>12</sub> prepared by sol-gel self combustion method. <i>Journal of Materials Science: Materials in Electronics</i> , <b>2012</b> , 23, 692-696	2.1	12
445	Effect of MgO Nano-oxide Additions on the Superconductivity and Dielectric Properties of Cu <sub>0.25</sub> Ti <sub>0.75</sub> Ba <sub>2</sub> Ca <sub>3</sub> Cu <sub>4</sub> O <sub>12</sub> Superconducting Phase. <b>2012</b> , 25, 45-53		18
444	Enhancement of electrical conductivity and dielectric constant in Sn-doped nanocrystalline CoFe <sub>2</sub> O <sub>4</sub> . <b>2013</b> , 15, 1		12
443	The synthesis of monodispersed AgBiS <sub>2</sub> quantum dots with a giant dielectric constant. <b>2013</b> , 15, 7644		26
442	Electrical properties of rutile-type relaxor ferroelectric-like Fe <sub>0.9</sub> W <sub>0.05</sub> TiMO <sub>6</sub> (M = Ta,Nb) ceramics. <b>2013</b> , 30, 191-205		3
441	Electronic and magnetic reconstructions in manganite superlattices. <i>Physical Review B</i> , <b>2013</b> , 87,	3.3	9
440	Size and Lone Pair Effects on the Multiferroic Properties of Bi <sub>0.75</sub> A <sub>0.25</sub> FeO <sub>3</sub> (A = Sr, Pb, and Ba) Ceramics. <i>Journal of the American Ceramic Society</i> , <b>2013</b> , 96, 3141-3148	3.8	35
439	Change of Mott variable range to small polaronic hole hopping conduction mechanism and formation of Schottky barriers in Nd <sub>0.9</sub> Sr <sub>0.1</sub> FeO <sub>3</sub> . <i>Journal of Applied Physics</i> , <b>2013</b> , 114, 034103	2.5	25
438	Effects of substrate temperature and ambient oxygen pressure on growth of Ba(Fe <sub>1/2</sub> Nb <sub>1/2</sub> )O <sub>3</sub> thin films by pulsed laser deposition. <b>2013</b> , 58, 3398-3402		7

437	Preparation and functional characterization of BiFeO <sub>3</sub> ceramics: A comparative study of the dielectric properties. <b>2013</b> , 23, 79-87		18
436	Intrinsic electrical properties of LuFe <sub>2</sub> O <sub>4</sub> . <i>Physical Review B</i> , <b>2013</b> , 88,	3-3	44
435	Polar and magnetic layered A-site and rock salt B-site-ordered NaLnFeWO <sub>6</sub> (Ln = La, Nd) perovskites. <b>2013</b> , 52, 12482-91		21
434	Applications of CCTO supercapacitor in energy storage and electronics. <b>2013</b> , 3, 062126		60
433	Dielectric behaviors and high energy storage density of nanocomposites with core-shell BaTiO <sub>3</sub> @TiO <sub>2</sub> in poly(vinylidene fluoride-hexafluoropropylene). <b>2013</b> , 15, 16242-8		128
432	Low dimensional fabrication of giant dielectric CaCu <sub>3</sub> Ti <sub>4</sub> O <sub>12</sub> through soft e-beam lithography. <i>Journal of Alloys and Compounds</i> , <b>2013</b> , 547, 147-151	5-7	12
431	Effect of strain and grain boundaries on dielectric properties in La <sub>0.7</sub> Sr <sub>0.3</sub> MnO <sub>3</sub> thin films. <b>2013</b> , 48, 2115-2122		14
430	Microstructures and dielectric relaxation behaviors of pure and tellurium doped CaCu <sub>3</sub> Ti <sub>4</sub> O <sub>12</sub> ceramics prepared via vibro-milling method. <i>Ceramics International</i> , <b>2013</b> , 39, S359-S364	5-1	5
429	Dielectric properties of Zr doped CaCu <sub>3</sub> Ti <sub>4</sub> O <sub>12</sub> synthesized by sol-gel route. <i>Journal of Alloys and Compounds</i> , <b>2013</b> , 551, 456-462	5-7	36
428	Dielectric abnormalities in complex perovskite BaTi <sub>1-x</sub> (Co <sub>0.5</sub> Nb <sub>0.5</sub> ) <sub>x</sub> O <sub>3</sub> ceramics. <b>2013</b> , 106, 366-368		6
427	Dielectric, modulus and impedance spectroscopic studies of nanostructured CaCu <sub>2.7</sub> Mg <sub>0.3</sub> Ti <sub>4</sub> O <sub>12</sub> electro-ceramic synthesized by modified sol-gel route. <i>Journal of Alloys and Compounds</i> , <b>2013</b> , 555, 176-183	5-7	41
426	Dielectric relaxation behaviour of Li and La co-doped NiO ceramics. <i>Ceramics International</i> , <b>2013</b> , 39, 4263-4268	5-1	27
425	Extraction and dielectric properties of curcuminoid films grown on Si substrate for high-k dielectric applications. <b>2013</b> , 178, 1062-1067		3
424	Soft mode in cubic PbTiO <sub>3</sub> by hyper-Raman scattering. <i>Physical Review B</i> , <b>2013</b> , 87,	3-3	8
423	Significant enhancements of dielectric and magnetic properties in Bi(Fe <sub>1-x</sub> Mgx)O <sub>3-x/2</sub> induced by oxygen vacancies. <b>2013</b> , 46, 145001		27
422	Dielectric properties of Ge <sub>2</sub> Sb <sub>2</sub> Te <sub>5</sub> phase-change films. <i>Journal of Applied Physics</i> , <b>2013</b> , 113, 113705	2-5	13
421	Enhanced dielectric properties of BaTiO <sub>3</sub> /poly(vinylidene fluoride) nanocomposites for energy storage applications. <i>Journal of Applied Physics</i> , <b>2013</b> , 113, 034105	2-5	168
420	Poly(vinylidene fluoride) polymer based nanocomposites with significantly reduced energy loss by filling with core-shell structured BaTiO <sub>3</sub> /SiO <sub>2</sub> nanoparticles. <b>2013</b> , 102, 102903		143

4 <sup>19</sup>	Structural, transport, magnetic, and dielectric properties of $\text{La}_{1-x}\text{Te}_x\text{MnO}_3$ ( $x = 0.10$ and $0.15$ ). <b>2013</b> , 48, 3272-3282		9
4 <sup>18</sup>	Electron-pinned defect-dipoles for high-performance colossal permittivity materials. <b>2013</b> , 12, 821-6		541
4 <sup>17</sup>	Hydrothermal synthesis, characterization and electrical investigation of poly(para-phenylenediamine)/vanadium oxide nanocomposite nanosheets. <b>2013</b> , 178, 502-510		9
4 <sup>16</sup>	Magnetic and dielectric properties of quasi-two-dimensional manganese oxide $\text{Sr}_7\text{Mn}_4\text{O}_{15}$ . <i>Journal of Magnetism and Magnetic Materials</i> , <b>2013</b> , 328, 66-71	2.8	5
4 <sup>15</sup>	Effect of sintering in oxygen on electrical conduction and dielectric properties in $\text{CaCu}_3\text{Ti}_4\text{O}_{12}$ . <i>Materials Research Bulletin</i> , <b>2013</b> , 48, 310-314	5.1	21
4 <sup>14</sup>	Dielectric behavior of $\text{CaCu}_3\text{Ti}_4\text{O}_{12}$ electro-ceramic doped with La, Mn and Ni synthesized by modified citrate-gel route. <b>2013</b> , 2, 119-127		6
4 <sup>13</sup>	Colossal Permittivity and Variable-Range-Hopping Conduction of Polarons in $\text{Ni}_{0.5}\text{Zn}_{0.5}\text{Fe}_2\text{O}_4$ Ceramic. <b>2013</b> , 117, 12966-12972		57
4 <sup>12</sup>	Dielectric response and magnetoelectric coupling in single crystal gallium ferrite. <b>2013</b> , 3, 052115		14
4 <sup>11</sup>	Tunable dielectric and ferroelectric properties in heteroepitaxial $\text{PbZr}_{0.52}\text{Ti}_{0.48}\text{O}_3/\text{La}_{0.625}\text{Ca}_{0.375}\text{MnO}_3$ thin films. <i>Journal of Applied Physics</i> , <b>2013</b> , 114, 034102	2.5	10
4 <sup>10</sup>	Electron Paramagnetic Resonance Probed Defects in the Colossal Dielectric Constant Perovskite $\text{CaCu}_3\text{Ti}_4\text{O}_{12}$ . <b>2013</b> , 82, 064707		7
4 <sup>09</sup>	Colossal dielectric constant polymer nanocomposites: Role of charge injection at matrix/filler interfaces. <b>2013</b> , 47, 2353-2360		1
4 <sup>08</sup>	Charge carriers and small-polaron migration as the origin of intrinsic dielectric anomalies in multiferroic $\text{TbMnO}_3$ polycrystals. <i>Journal of Physics Condensed Matter</i> , <b>2013</b> , 25, 475401	1.8	8
4 <sup>07</sup>	Fabrication, structure, and property of epoxy-based composites with metal-insulator core-shell structure fillers. <b>2013</b> , 28, 2644-2649		11
4 <sup>06</sup>	Influence of LNO Top Electrodes on Electrical Properties of KNN/LNO Thin Films Prepared by RF Magnetron Sputtering. <i>Journal of the American Ceramic Society</i> , <b>2013</b> , 96, 787-790	3.8	29
4 <sup>05</sup>	Dielectric and Magnetic Properties of $\text{Sr}(\text{Fe}_{1/2}\text{Ta}_{1/2})\text{O}_3$ Complex Perovskite Ceramics. <i>Journal of the American Ceramic Society</i> , <b>2013</b> , 96, 1188-1192	3.8	7
4 <sup>04</sup>	Anomalous change in dielectric constant of $\text{CaCu}_3\text{Ti}_4\text{O}_{12}$ under violet-to-ultraviolet irradiation. <b>2013</b> , 102, 202903		19
4 <sup>03</sup>	Structural characterization and observation of variable range hopping conduction mechanism at high temperature in CdSe quantum dot solids. <i>Journal of Applied Physics</i> , <b>2013</b> , 113, 093703	2.5	12
4 <sup>02</sup>	Optical probe of ferroelectric order in bulk and thin-film perovskite titanates. <i>Physical Review B</i> , <b>2013</b> , 88,	3.3	28

401	Effect of TeO <sub>2</sub> addition on the dielectric properties of CaCu <sub>3</sub> Ti <sub>4</sub> O <sub>12</sub> ceramics derived from the oxalate precursor route. <b>2013</b> , 03, 1350028		1
400	Origin of the colossal dielectric properties in double-perovskite Sr <sub>2</sub> CoNbO <sub>6</sub> . <b>2013</b> , 3, 022109		18
399	Effect of Different Preparing Methods on the Microstructures and Dielectric Relaxation Behaviors of CaCu <sub>3</sub> Ti <sub>4</sub> O <sub>12</sub> Ceramics. <b>2013</b> , 456, 120-127		2
398	Ferroelectric/ferromagnetic ceramic composite and its hybrid permittivity stemming from hopping charge and conductivity inhomogeneity. <i>Journal of Applied Physics</i> , <b>2013</b> , 113, 044101	2.5	40
397	Distinctive contributions to dielectric response of relaxor ferroelectric lead scandium niobate ceramic system. <b>2013</b> , 250, 2232-2236		9
396	Femtosecond tunneling of polarons in Pb <sub>5</sub> Cr <sub>3</sub> F <sub>19</sub> . <b>2014</b> , 04, 1450020		
395	Oxygen vacancy induced dielectric relaxation studies in Bi <sub>4-x</sub> La <sub>x</sub> Ti <sub>3</sub> O <sub>12</sub> (x = 0.0, 0.3, 0.7, 1.0) ceramics. <i>Journal of Materials Science: Materials in Electronics</i> , <b>2014</b> , 25, 4568-4576	2.1	15
394	Super Dielectric Materials. <b>2014</b> , 7, 8197-8212		21
393	Domain dynamics in the multiferroic phase of MnWO <sub>4</sub> . <i>Physical Review B</i> , <b>2014</b> , 89,	3.3	15
392	Giant dielectric constant in TiO <sub>2</sub> /Al <sub>2</sub> O <sub>3</sub> nanolaminates grown on doped silicon substrate by pulsed laser deposition. <i>Journal of Applied Physics</i> , <b>2014</b> , 115, 094103	2.5	17
391	Giant dielectric tunability properties of Sr and Sb co-doped La <sub>2</sub> NiMnO <sub>6</sub> ceramics induced by extrinsic contribution. <i>Physica Status Solidi (A) Applications and Materials Science</i> , <b>2014</b> , 211, 1207-1212	1.6	10
390	Ionic mobility in DNA films studied by dielectric spectroscopy. <b>2014</b> , 37, 39		1
389	Tuning of colossal dielectric constant in gold-polypyrrole composite nanotubes using in-situ x-ray diffraction techniques. <b>2014</b> , 4, 097121		4
388	Large dielectric permittivity and possible correlation between magnetic and dielectric properties in bulk BaFeO <sub>3</sub> . <b>2014</b> , 105, 042906		31
387	A comparative study of structural, magnetic, dielectric behaviors and impedance spectroscopy for bulk and nanometric double perovskite Sm <sub>2</sub> CoMnO <sub>6</sub> . <b>2014</b> , 1, 046108		11
386	Dielectric and conducting behaviour of polycrystalline holmium octa-molybdate. <b>2014</b> , 1, 035030		
385	Dielectric properties of CaCu <sub>3</sub> Ti <sub>4</sub> O <sub>12</sub> ceramics with Zn substitution for Cu. <b>2014</b> , 113, 98-101		2
384	Converse electrostrictive effect in dielectric polymers. <b>2014</b> , 190, 259-264		16



383	Microwave absorption properties of dielectric La <sub>1.5</sub> Sr <sub>0.5</sub> NiO <sub>4</sub> ultrafine particles. <b>2014</b> , 186, 101-105		13
382	Effects of Kaolinite additions on sintering behavior and dielectric properties of CaCu <sub>3</sub> Ti <sub>4</sub> O <sub>12</sub> ceramics. <i>Journal of Materials Science: Materials in Electronics</i> , <b>2014</b> , 25, 546-551	2.1	7
381	High dielectric permittivity of Li and Sc co-doped NiO ceramics. <i>Journal of Materials Science: Materials in Electronics</i> , <b>2014</b> , 25, 1298-1302	2.1	8
380	Dielectric properties of Y <sub>2</sub> O <sub>3</sub> donor-doped Ba <sub>0.8</sub> Sr <sub>0.2</sub> TiO <sub>3</sub> ceramics. <i>Materials Chemistry and Physics</i> , <b>2014</b> , 143, 676-680	4.4	5
379	Large enhanced dielectric permittivity in polyaniline passivated core-shell nano magnetic iron oxide by plasma polymerization. <b>2014</b> , 104, 121603		20
378	Polaronic phase transitions and complex permittivity of solid polar insulators with gigantic dielectric response. <b>2014</b> , 251, 569-592		2
377	Dielectric and electrical studies of Pr <sup>3+</sup> doped nano CaSiO <sub>3</sub> perovskite ceramics. <i>Materials Research Bulletin</i> , <b>2014</b> , 50, 197-202	5.1	24
376	Possible Piezoelectric Materials CsMZr <sub>0.5</sub> (MoO <sub>4</sub> ) <sub>3</sub> (M = Al, Sc, V, Cr, Fe, Ga, In) and CsCrTi <sub>0.5</sub> (MoO <sub>4</sub> ) <sub>3</sub> : Structure and Physical Properties. <b>2014</b> , 118, 1763-1773		23
375	Poly(vinylidene fluoride) polymer based nanocomposites with enhanced energy density by filling with polyacrylate elastomers and BaTiO <sub>3</sub> nanoparticles. <b>2014</b> , 104, 082904		36
374	Electrodynamics properties of lead Zirconate-Titanate thin films in the terahertz frequency range. <b>2014</b> , 56, 2206-2212		6
373	Dielectric Change of Copper Phthalocyanine and Polyurethane Foam with High Elasticity as a Function of Pressure Discussed in Terms of Conversion from Natural Mechanical Energy to Electric Energy. <b>2014</b> , 47, 8281-8294		4
372	Atmosphere controlled conductivity and Maxwell-Wagner relaxation in Bi <sub>0.5</sub> K <sub>0.5</sub> TiO <sub>3</sub> BiFeO <sub>3</sub> ceramics. <i>Journal of Applied Physics</i> , <b>2014</b> , 115, 044104	2.5	33
371	A colossal dielectric constant of an amorphous TiO <sub>2</sub> :(Nb, In) film with low loss fabrication at room temperature. <b>2014</b> , 2, 6790-6795		78
370	High pressure treated ZnO ceramics towards giant dielectric constants. <b>2014</b> , 2, 16740-16745		27
369	Strong spin-phonon coupling in infrared and Raman spectra of SrMnO <sub>3</sub> . <i>Physical Review B</i> , <b>2014</b> , 89,	3.3	37
368	High dielectric constant response of modified copper phthalocyanine. <b>2014</b> , 199, 324-329		13
367	Effects of A-site disorder in the properties of A <sub>2</sub> CoMnO <sub>6</sub> (A = La, Tb). <i>Journal of Physics Condensed Matter</i> , <b>2014</b> , 26, 386001	1.8	13
366	Magnetodielectric behaviour in La <sub>0.53</sub> Ca <sub>0.47</sub> MnO <sub>3</sub> . <b>2014</b> , 47, 435303		6



365	Photoinduced Giant Dielectric Constant in Lead Halide Perovskite Solar Cells. <b>2014</b> , 5, 2390-4		551
364	Electrical properties of rutile-type $\text{In}(\text{Al})_{0.025}\text{Nb}_{0.025}\text{Ti}_{0.95}\text{O}_2$ ceramics. <b>2014</b> , 33, 163-171		3
363	Enhanced energy storage density in poly(vinylidene fluoride) nanocomposites by a small loading of surface-hydroxylated $\text{Ba}_{0.6}\text{Sr}_{0.4}\text{TiO}_3$ nanofibers. <b>2014</b> , 6, 1533-40		179
362	Polymer Nanocomposites with High Permittivity. <b>2014</b> , 305-333		4
361	Magnetoelectric properties of laminated $\text{La}_{0.7}\text{Ba}_{0.3}\text{MnO}_3/\text{BaTiO}_3$ ceramic composites. <i>Journal of Magnetism and Magnetic Materials</i> , <b>2014</b> , 364, 18-23	2.8	17
360	Leading role of grain boundaries in colossal permittivity of doped and undoped CCTO. <b>2014</b> , 34, 3649-3654		70
359	Impedance spectroscopic investigation of electro active regions, conduction mechanism and origin of colossal dielectric constant in $\text{Nd}_{1-x}\text{Sr}_x\text{FeO}_3$ (0.1 $\leq$ x $\leq$ 0.5). <i>Materials Research Bulletin</i> , <b>2014</b> , 60, 474-484	5.1	22
358	Effects of praseodymium substitution on electrical properties of $\text{CaCu}_3\text{Ti}_4\text{O}_{12}$ ceramics. <i>Ceramics International</i> , <b>2014</b> , 40, 181-189	5.1	13
357	Giant gigahertz optical activity in multiferroic ferroborate. <i>Physical Review B</i> , <b>2014</b> , 89,	3.3	22
356	Anomalous electrical transport properties of CdSe quantum dots at and below room temperature. <i>Physica B: Condensed Matter</i> , <b>2014</b> , 438, 70-77	2.8	17
355	Dielectric properties of the spin-1/2 dimer compounds $\text{Ba}_3\text{Cr}_2\text{O}_8$ and $\text{Sr}_3\text{Cr}_2\text{O}_8$ . <i>Materials Chemistry and Physics</i> , <b>2014</b> , 145, 461-464	4.4	
354	Progress in the growth of $\text{CaCu}_3\text{Ti}_4\text{O}_{12}$ and related functional dielectric perovskites. <b>2014</b> , 60, 15-62		84
353	Role of Annealing Atmosphere on Structure, Dielectric and Magnetic Properties of $\text{La}_2\text{CoMnO}_6$ and $\text{La}_2\text{MgMnO}_6$ . <b>2014</b> , 640, 1907-1921		23
352	Complex diffusion behavior of oxygen in nanocrystalline $\text{BaTiO}_3$ ceramics. <b>2014</b> , 16, 2568-75		14
351	Evidence of the charge-density wave state in polypyrrole nanotubes. <i>Physical Review B</i> , <b>2015</b> , 91,	3.3	5
350	Crystal structure, incommensurate magnetic order, and ferroelectricity in $\text{Mn}_{1-x}\text{Cu}_x\text{WO}_4$ (0 $\leq$ x $\leq$ 0.19). <i>Physical Review B</i> , <b>2015</b> , 91,	3.3	11
349	Ferroelectric properties of charge-ordered $\text{Bi}(\text{BEDTTF})_2\text{I}_3$ . <i>Physical Review B</i> , <b>2015</b> , 91,	3.3	27
348	Ferromagnetism and the effect of free charge carriers on electric polarization in the double perovskite $\text{Y}_2\text{NiMnO}_6$ . <i>Physical Review B</i> , <b>2015</b> , 92,	3.3	28

347	Ferroelectricity in underdoped La-based cuprates. <b>2015</b> , 5, 15268		5
346	Magnetocapacitance effects in MnZn ferrites. <b>2015</b> , 5, 117130		8
345	Microstructure and electric characteristics of AETiO <sub>3</sub> (AE=Mg, Ca, Sr) doped CaCu <sub>3</sub> Ti <sub>4</sub> O <sub>12</sub> thin films prepared by the sol-gel method. <b>2015</b> , 25, 399-404		8
344	Structural and Dielectric Properties of Subnanometric Laminates of Binary Oxides. <b>2015</b> , 7, 25679-84		7
343	Tube-Super Dielectric Materials: Electrostatic Capacitors with Energy Density Greater than 200 J/cm <sup>3</sup> . <b>2015</b> , 8, 6208-6227		12
342	Origin of magnetocapacitance in chemically homogeneous and inhomogeneous ferrites. <b>2015</b> , 17, 2432-7		8
341	Giant dielectric response and low dielectric loss in Al <sub>2</sub> O <sub>3</sub> grafted CaCu <sub>3</sub> Ti <sub>4</sub> O <sub>12</sub> ceramics. <i>Journal of Applied Physics</i> , <b>2015</b> , 117, 094103	2.5	19
340	The manifestation of spin-phonon coupling in CaMnO <sub>3</sub> . <i>Journal of Applied Physics</i> , <b>2015</b> , 117, 164103	2.5	9
339	Electrical properties and Mössbauer spectra of rutile-type Fe <sub>x/2</sub> Ta(Nb) <sub>x/2</sub> Ti <sub>1-x</sub> O <sub>2</sub> (x = 0.05, 0.1) ceramics. <b>2015</b> , 34, 158-166		1
338	Processing of dielectric oxynitride perovskites for powders, ceramics, compacts and thin films. <b>2015</b> , 44, 10570-81		32
337	Multiferroicity and skyrmions carrying electric polarization in GaV <sub>4</sub> S <sub>8</sub> . <b>2015</b> , 1, e1500916		100
336	FeCr <sub>2</sub> In magnetic fields: possible evidence for a multiferroic ground state. <b>2014</b> , 4, 6079		24
335	High dielectric permittivity and low dielectric loss in sol-gel derived Zn doped CaCu <sub>3</sub> Ti <sub>4</sub> O <sub>12</sub> thin films. <i>Materials Chemistry and Physics</i> , <b>2015</b> , 153, 229-235	4.4	34
334	Effect of in situ synthesized Fe <sub>2</sub> O <sub>3</sub> and Co <sub>3</sub> O <sub>4</sub> nanoparticles on electroactive phase crystallization and dielectric properties of poly(vinylidene fluoride) thin films. <b>2015</b> , 17, 1368-78		82
333	Electrical properties of AC <sub>3</sub> B <sub>4</sub> O <sub>12</sub> -type perovskite ceramics with different cation vacancies. <i>Materials Research Bulletin</i> , <b>2015</b> , 65, 260-265	5.1	33
332	Novel Materials with Effective Super Dielectric Constants for Energy Storage. <b>2015</b> , 44, 1367-1376		9
331	Interfacial capacitance between a ferroelectric Fe <sub>3</sub> O <sub>4</sub> thin film and a semiconducting Nb:SrTiO <sub>3</sub> substrate. <i>Journal of Applied Physics</i> , <b>2015</b> , 117, 014104	2.5	9
330	Oxygen vacancy related defect dipoles in CaCu <sub>3</sub> Ti <sub>4</sub> O <sub>12</sub> : Detected by electron paramagnetic resonance spectroscopy. <b>2015</b> , 35, 2073-2081		38

329	Cu-PDC-bpa solid coordination frameworks (PDC=2,5-pyrindinedicarboxylate; bpa=1,2-DI(4-pyridil)ethane): 2D and 3D structural flexibility producing a 3-c herringbone array next to ideal. <b>2015</b> , 230, 191-198		4
328	Improvement of electroactive phase nucleation and dielectric properties of WO <sub>3</sub> ·H <sub>2</sub> O nanoparticle loaded poly(vinylidene fluoride) thin films. <b>2015</b> , 5, 62819-62827		33
327	Structural and optical properties of Ni substituted CaCu <sub>3</sub> Ti <sub>4</sub> ·xNi <sub>x</sub> O <sub>12</sub> . <b>2015</b> , 126, 3437-3441		7
326	Microwave Response of Conducting Na <sub>x</sub> CoO <sub>2</sub> ·yH <sub>2</sub> O Nanoparticles. <b>2015</b> , 119, 13957-13964		2
325	Capacitance scaling of grain boundaries with colossal permittivity of CaCu <sub>3</sub> Ti <sub>4</sub> O <sub>12</sub> -based materials. <b>2015</b> , 42, 25-29		17
324	Relation between the microstructure and the electromagnetic properties of BaTiO <sub>3</sub> /Ni <sub>0.5</sub> Zn <sub>0.5</sub> Fe <sub>2</sub> O <sub>4</sub> ceramic composite. <i>Applied Physics A: Materials Science and Processing</i> , <b>2015</b> , 119, 1291-1300	2.6	13
323	In situ synthesis of Ni(OH) <sub>2</sub> nanobelt modified electroactive poly(vinylidene fluoride) thin films: remarkable improvement in dielectric properties. <b>2015</b> , 17, 13082-91		72
322	The expanding world of hybrid perovskites: materials properties and emerging applications. <b>2015</b> , 5, 7-26		105
321	Electrical transport in titania nanoparticles embedded in conducting polymer matrix. <b>2015</b> , 4,		5
320	Magnetic Behaviors of Mg- and Zn-Doped Fe <sub>3</sub> O <sub>4</sub> Nanoparticles Estimated in Terms of Crystal Domain Size, Dielectric Response, and Application of Fe <sub>3</sub> O <sub>4</sub> /Carbon Nanotube Composites to Anodes for Lithium Ion Batteries. <b>2015</b> , 119, 26128-26142		22
319	Low temperature magneto-dielectric measurements on BiFeO <sub>3</sub> lightly substituted by cobalt. <i>Journal of Applied Physics</i> , <b>2015</b> , 117, 134102	2.5	12
318	Structural, magnetic and electrical properties of Bi doped LaFeO <sub>3</sub> nano-crystals, synthesized by auto-combustion method. <i>Journal of Materials Science: Materials in Electronics</i> , <b>2015</b> , 26, 8765-8773	2.1	23
317	Dielectric spectroscopy on organic charge-transfer salts. <i>Journal of Physics Condensed Matter</i> , <b>2015</b> , 27, 373001	1.8	24
316	Origin of colossal permittivity in (In <sub>1/2</sub> Nb <sub>1/2</sub> )TiO <sub>2</sub> via broadband dielectric spectroscopy. <b>2015</b> , 17, 23132-9		42
315	Enhanced extrinsic dielectric response of TiO <sub>2</sub> modified CaCu <sub>3</sub> Ti <sub>4</sub> O <sub>12</sub> ceramics. <i>Ceramics International</i> , <b>2015</b> , 41, 13447-13454	5.1	34
314	Electrical transport properties of polyvinyl alcohol·selenium nanocomposite films at and above room temperature. <b>2015</b> , 50, 1632-1645		32
313	Bismuth centred magnetic perovskite: A projected multiferroic. <i>Journal of Magnetism and Magnetic Materials</i> , <b>2015</b> , 378, 506-528	2.8	14
312	Correlation between structure, oxygen content and the multiferroic properties of Sr doped BiFeO <sub>3</sub> . <i>Journal of Alloys and Compounds</i> , <b>2015</b> , 622, 8-16	5.7	69

311	Dielectric characterization of a nonlinear optical material. <b>2014</b> , 4, 6020		10
310	Crucial role of percolation transition on the formation and electromagnetic properties of BaTiO <sub>3</sub> /Ni <sub>0.5</sub> Zn <sub>0.47</sub> Fe <sub>2</sub> O <sub>4</sub> ceramic composites. <i>Ceramics International</i> , <b>2015</b> , 41, 1511-1519	5.1	8
309	Piezoelectric and dielectric properties of PZT/elemental aluminum nano-composites. <i>Ceramics International</i> , <b>2015</b> , 41, 819-833	5.1	16
308	Investigation of Fumed Silica/Aqueous NaCl Superdielectric Material. <b>2016</b> , 9,		6
307	Novel Superdielectric Materials: Aqueous Salt Solution Saturated Fabric. <b>2016</b> , 9,		6
306	Growth, composition, ferroelectric and magnetic properties of new multiferroic Pb <sub>3.3</sub> Mn <sub>4.8</sub> Ni <sub>1.1</sub> Ti <sub>0.56</sub> O <sub>15.3</sub> single crystals. <b>2016</b> , 51, 446-452		0
305	Magnetically controlled space charge capacitance at La <sub>1-x</sub> Sr <sub>x</sub> MnO <sub>3</sub> /Sr <sub>x</sub> La <sub>1-x</sub> TiO <sub>3</sub> interfaces. <i>Physica Status Solidi (A) Applications and Materials Science</i> , <b>2016</b> , 213, 2243-2253	1.6	1
304	Colossal dielectric constant in high entropy oxides. <b>2016</b> , 10, 328-333		279
303	Dielectric relaxation and polaronic hopping in Mn-substituted LaSrNiO <sub>4</sub> nickelates prepared by mechanical milling method. <i>Journal of Alloys and Compounds</i> , <b>2016</b> , 688, 163-172	5.7	6
302	Structural, magnetic, and electrical features of the Nd <sub>2</sub> SrMn <sub>2</sub> TiO <sub>9</sub> perovskite-like compound. <b>2016</b> , 253, 1127-1132		1
301	Magnetoelectric phase diagrams of multiferroic GdMn <sub>2</sub> O <sub>5</sub> . <i>Physical Review B</i> , <b>2016</b> , 94,	3.3	17
300	Morphology-dependent space charge polarization and dielectric relaxation of CdO nanomorphotypes. <b>2016</b> , 06, 1650030		3
299	Dielectric and ferroelectric study of La <sub>5</sub> Ti <sub>4</sub> O <sub>15</sub> synthesised by semi-wet route. <b>2016</b> , 5, 113-117		1
298	Origin of magnetic and dielectric response in single phase nano crystalline BiFeO <sub>3</sub> . <b>2016</b> , 3, 125015		2
297	Charge Transport in Antiferromagnetic Insulating Phase of Two-Dimensional Organic Conductor [(BETS) <sub>2</sub> FeCl <sub>4</sub> ]. <b>2016</b> , 85, 064703		7
296	Study of structural, electrical, and dielectric properties of phosphate-borate glasses and glass-ceramics. <i>Journal of Applied Physics</i> , <b>2016</b> , 120, 051701	2.5	9
295	Direct view at colossal permittivity in donor-acceptor (Nb, In) co-doped rutile TiO <sub>2</sub> . <b>2016</b> , 109, 092906		43
294	Hybrid Cluster Precursors of the LaZrO Insulator for Transistors: Properties of High-Temperature-Processed Films and Structures of Solutions, Gels, and Solids. <b>2016</b> , 6, 29682		9

293	Piezoelectric response of BiFeO <sub>3</sub> ceramics at elevated temperatures. <b>2016</b> , 109, 042904		34
292	Transport mechanism through metal-cobaltite interfaces. <b>2016</b> , 109, 011603		17
291	Electrode effects in dielectric spectroscopy measurements on (Nb+In) co-doped TiO <sub>2</sub> . <i>Journal of Applied Physics</i> , <b>2016</b> , 119, 154105	2.5	26
290	Dielectric characterization of multiferroic magnetoelectric double-perovskite Y(Ni <sub>0.5</sub> Mn <sub>0.5</sub> )O <sub>3</sub> thin films. <b>2016</b> , 109, 152901		6
289	Complex permittivity and relaxation processes in CaCu <sub>3</sub> Ti <sub>4</sub> MnO <sub>12</sub> . <i>Ceramics International</i> , <b>2016</b> , 42, 10866-10871	5.1	7
288	Microwave Dielectric Properties of Ca <sub>1+x</sub> Cu <sub>3</sub> Ti <sub>4</sub> O <sub>12+x</sub> (-0.04 ≤ x ≤ 0.04) Ceramics. <b>2016</b> , 19, 929-934		6
287	Phase structure, microstructure and broadband dielectric response of Cu nonstoichiometry CaCu <sub>3</sub> Ti <sub>4</sub> O <sub>12</sub> ceramic. <i>Journal of Alloys and Compounds</i> , <b>2016</b> , 683, 579-589	5.7	18
286	Internal barrier layer capacitor, nearest neighbor hopping, and variable range hopping conduction in Ba <sub>1-x</sub> Sr <sub>x</sub> TiO <sub>3</sub> nanoceramics. <b>2016</b> , 51, 7440-7450		9
285	EFFECTS OF ELECTRODE RESISTANCE ON THE DIELECTRIC BEHAVIORS OF Au/BaxSr <sub>1-x</sub> TiO <sub>3</sub> /La <sub>1.1</sub> Sr <sub>0.9</sub> NiO <sub>4</sub> CAPACITORS. <b>2016</b> , 23, 1650028		0
284	Tuning of dielectric properties of (ZnO)-(CuTi-1223) nanoparticles-superconductor composites. <i>Ceramics International</i> , <b>2016</b> , 42, 11193-11200	5.1	8
283	Mechanically strong, flexible and thermally stable graphene oxide/nanocellulosic films with enhanced dielectric properties. <b>2016</b> , 6, 49138-49149		51
282	Calcium Copper Titanate Based High Dielectric Constant Materials for Energy Storage Applications. <b>2016</b> , 131-140		2
281	Impact of water on the charge transport of a glass-forming ionic liquid. <b>2016</b> , 223, 635-642		14
280	Central role of TiO <sub>2</sub> anatase grain boundaries on resistivity of CaCu <sub>3</sub> Ti <sub>4</sub> O <sub>12</sub> -based materials probed by Raman spectroscopy. <b>2016</b> , 61, 102-105		15
279	Direct Current Conductivity of Thin-Film Ionic Conductors from Analysis of Dielectric Spectroscopic Measurements in Time and Frequency Domains. <b>2016</b> , 120, 21254-21262		1
278	Testing the Tube Super-Dielectric Material Hypothesis: Increased Energy Density Using NaCl. <b>2016</b> , 45, 5499-5506		6
277	Features of the low-frequency polarization response in the region of the ferroelectric phase transition in multiferroic TbMnO <sub>3</sub> . <b>2016</b> , 58, 2021-2026		1
276	Nanolaminated composite materials: structure, interface role and applications. <b>2016</b> , 6, 109361-109385		37

275	Impedance Characteristics of Hybrid Organometal Halide Perovskite Solar Cells. <b>2016</b> , 163-199		8
274	Dynamics of electron density, spin-phonon coupling, and dielectric properties of SmFeO <sub>3</sub> nanoparticles at the spin-reorientation temperature: Role of exchange striction. <i>Physical Review B</i> , <b>2016</b> , 93,	3-3	47
273	Magnetoelectric and structural properties of Y <sub>2</sub> CoMnO <sub>6</sub> : The role of antisite defects. <i>Physical Review B</i> , <b>2016</b> , 93,	3-3	32
272	Dielectric relaxations in Ba <sub>0.85</sub> Sr <sub>0.15</sub> TiO <sub>3</sub> thin films deposited on Pt/Ti/SiO <sub>2</sub> /Si substrates by sol-gel method. <i>Journal of Materials Science: Materials in Electronics</i> , <b>2016</b> , 27, 11299-11307	2-1	12
271	High Pressure Experimental Studies on CuO: Indication of Re-entrant Multiferroicity at Room Temperature. <b>2016</b> , 6, 31610		26
270	Magnetocapacitance effect in Gd x Mn <sub>1-x</sub> S. <b>2016</b> , 58, 1148-1153		3
269	Poling-Written Ferroelectricity in Bulk Multiferroic Double-Perovskite BiFe <sub>0.5</sub> Mn <sub>0.5</sub> O <sub>3</sub> . <b>2016</b> , 55, 6308-14		11
268	Conducting polyaniline-rutile TiO <sub>2</sub> nanocomposites for the development of high-k dielectric materials. <b>2016</b> , 14, 238-243		2
267	Magnetodielectric effect of Mn <sub>2</sub> N ferrite at resonant frequency. <i>Journal of Magnetism and Magnetic Materials</i> , <b>2016</b> , 416, 256-260	2-8	9
266	Crosslinked P(VDF-CTFE)/PS-COOH nanocomposites for high-energy-density capacitor application. <b>2016</b> , 54, 1160-1169		22
265	Colossal dielectric constant of NaNbO <sub>3</sub> doped BaTiO <sub>3</sub> ceramics. <b>2016</b> , 34, 322-329		12
264	Photoluminescence emission in zirconium-doped calcium copper titanate powders. <i>Ceramics International</i> , <b>2016</b> , 42, 4837-4844	5-1	5
263	Effect of doping ions on the structural defect and the electrical behavior of CaCu <sub>3</sub> Ti <sub>4</sub> O <sub>12</sub> ceramics. <i>Materials Research Bulletin</i> , <b>2016</b> , 76, 124-132	5-1	26
262	Influence of FeNb codoping on the dielectric and electrical properties of CaCu <sub>3</sub> Ti <sub>4</sub> O <sub>12</sub> ceramics. <i>Journal of Alloys and Compounds</i> , <b>2016</b> , 661, 6-13	5-7	10
261	Observation of large dielectric permittivity and dielectric relaxation phenomenon in Mn-doped lanthanum gallate. <b>2016</b> , 6, 26621-26629		22
260	Thermally stable yttrium-cadmium oxide high-k dielectrics deposited by a solution process. <b>2016</b> , 49, 115109		18
259	Dielectric elastomers based on silicones filled with transitional metal complexes. <b>2016</b> , 93, 236-243		18
258	Strain-Dependent Dielectric Behavior of Carbon Black Reinforced Natural Rubber. <b>2016</b> , 49, 2339-2347		40

257	Structural, microstructural and dielectric studies in multiferroic LaSrNiO <sub>4-δ</sub> prepared by mechanical milling method. <i>Journal of Alloys and Compounds</i> , <b>2016</b> , 662, 467-474	5.7	19
256	Dielectric investigation of high-k yttrium copper titanate thin films. <b>2016</b> , 4, 1080-1087		12
255	Complex dielectric and impedance behavior of magnetoelectric Fe <sub>2</sub> TiO <sub>5</sub> . <i>Journal of Alloys and Compounds</i> , <b>2016</b> , 663, 289-294	5.7	49
254	Negative permittivity in Fe <sub>50</sub> Ni <sub>50</sub> /epoxy magnetic composite materials at high-frequency. <i>Materials Chemistry and Physics</i> , <b>2016</b> , 170, 113-117	4.4	10
253	High dielectric constant in Al-doped ZnO ceramics using high-pressure treated powders. <i>Journal of Alloys and Compounds</i> , <b>2016</b> , 657, 90-94	5.7	35
252	Origin of giant dielectric constant and conductivity behavior in Zn <sub>1-x</sub> Mg <sub>x</sub> O (0 ≤ x ≤ 0.1) ceramics. <i>Materials Research Bulletin</i> , <b>2016</b> , 74, 1-8	5.1	19
251	Effect of uniaxial stress on the dielectric properties of BaTiO <sub>3</sub> +0.1wt.%Eu <sub>2</sub> O <sub>3</sub> ceramics. <b>2017</b> , 90, 72-77		1
250	Large low-field magnetodielectric response in multiferroic Bi <sub>2</sub> NiMnO <sub>6</sub> thin film. <b>2017</b> , 50, 135006		5
249	Controlling the Electrical and Magnetoelectric Properties of Epitaxially Strained Sr <sub>1-x</sub> Ba <sub>x</sub> MnO <sub>3</sub> Thin Films. <b>2017</b> , 4, 1601040		12
248	Effect of Gd <sup>3+</sup> and Al <sup>3+</sup> on optical and dielectric properties of ZnO nanoparticle prepared by two-step hydrothermal method. <i>Ceramics International</i> , <b>2017</b> , 43, 6932-6941	5.1	32
247	Impact of Cu <sub>2</sub> O doping on high dielectric properties of CuO ceramics. <b>2017</b> , 17, 781-784		8
246	Synthesis and characterization of high-density B <sub>2</sub> O <sub>3</sub> -added forsterite ceramics. <i>Ceramics International</i> , <b>2017</b> , 43, 7172-7176	5.1	10
245	Magnetic ordering and dielectric relaxation in the double perovskite YBaCuFeO. <i>Journal of Physics Condensed Matter</i> , <b>2017</b> , 29, 145801	1.8	8
244	Conductivity Contrast and Tunneling Charge Transport in the Vortexlike Ferroelectric Domain Patterns of Multiferroic Hexagonal YMnO <sub>3</sub> . <b>2017</b> , 118, 036803		31
243	Decisive role of mixed-valence structure in colossal dielectric constant of LaFeO <sub>3</sub> . <i>Journal of the American Ceramic Society</i> , <b>2017</b> , 100, 3042-3049	3.8	18
242	Point-defect-induced colossal dielectric behavior in GaAs single crystals. <b>2017</b> , 7, 26130-26135		12
241	Comparative studies of pure, Sr-doped, Ni-doped and co-doped CaCu <sub>3</sub> Ti <sub>4</sub> O <sub>12</sub> ceramics: Enhancement of dielectric properties. <i>Journal of Alloys and Compounds</i> , <b>2017</b> , 717, 121-126	5.7	44
240	Enhanced dielectric behavior and ac electrical response in Gd-Mn-ZnO nanoparticles. <i>Journal of Alloys and Compounds</i> , <b>2017</b> , 726, 11-21	5.7	21



239	Graphical analysis of current-voltage characteristics in memristive interfaces. <i>Journal of Applied Physics</i> , <b>2017</b> , 121, 134502	2.5	14
238	Effects of temperature on conduction mechanism, ac electrical and dielectric properties of NdFe <sub>0.9</sub> Ni <sub>0.1</sub> O <sub>3</sub> by employing impedance spectroscopy. <b>2017</b> , 21, 3093-3101		5
237	Structural and electrical properties of Dy <sup>3+</sup> substituted NiFe <sub>2</sub> O <sub>4</sub> ceramics prepared from powders derived by combustion method. <i>Ceramics International</i> , <b>2017</b> , 43, 8378-8390	5.1	12
236	Morphology, thermal, mechanical and electrical insulation properties of poly(4-methyl-1-pentene)/poly(ethylene-co-vinyl alcohol)-coated TiO <sub>2</sub> nanocomposites. <b>2017</b> , 114, 268-279		4
235	Electromechanical properties of electrostrictive CeO <sub>2</sub> :Gd membranes: Effects of frequency and temperature. <b>2017</b> , 110, 142902		17
234	Study of structural, electrical and dielectric behavior of cadmium selenide quantum dots/polyaniline nanocomposites. <b>2017</b> , 59, 233-241		1
233	The Role of Field Electron Emission in Polypropylene/Aluminum Nanodielectrics Under High Electric Fields. <b>2017</b> , 9, 10106-10119		27
232	A novel all-organic DIPAB/PVDF composite film with high dielectric permittivity. <i>Journal of Materials Science: Materials in Electronics</i> , <b>2017</b> , 28, 9658-9666	2.1	8
231	Effect of nickel substitution on electrical and microstructural properties of CaCu <sub>3</sub> Ti <sub>4</sub> O <sub>12</sub> ceramic. <i>Journal of Alloys and Compounds</i> , <b>2017</b> , 698, 152-158	5.7	25
230	Topotactic Reduction toward a Noncentrosymmetric Deficient Perovskite Tb <sub>0.50</sub> Ca <sub>0.50</sub> Mn <sub>0.96</sub> O <sub>2.37</sub> with Ordered Mn Vacancies and Piezoelectric Behavior. <b>2017</b> , 29, 9840-9850		7
229	Multiple Interfacial FeO@BaTiO/P(VDF-HFP) Core-Shell-Matrix Films with Internal Barrier Layer Capacitor (IBLC) Effects and High Energy Storage Density. <b>2017</b> , 9, 40792-40800		36
228	Multiferroic properties of the Y <sub>2</sub> BiFe <sub>5</sub> O <sub>12</sub> garnet. <i>Journal of Applied Physics</i> , <b>2017</b> , 122, 134101	2.5	7
227	Relaxation dynamics and polydispersity associated with defects and ferroelectric correlations in Ba-doped EuTiO. <i>Journal of Physics Condensed Matter</i> , <b>2017</b> , 29, 465402	1.8	4
226	Experimental and theoretical elucidation of dielectric behavior of MgO-r-GO nanocomposites. <b>2017</b> , 80, 18-26		4
225	Excitations and relaxation dynamics in multiferroic GeV <sub>4</sub> Se <sub>8</sub> studied by terahertz and dielectric spectroscopy. <i>Physical Review B</i> , <b>2017</b> , 96,	3.3	5
224	Polar and magnetic order in GaV <sub>4</sub> Se <sub>8</sub> . <i>Physical Review B</i> , <b>2017</b> , 96,	3.3	21
223	Dielectric and ferroelectric properties of Ho-doped BiFeO <sub>3</sub> nanopowders across the structural phase transition. <i>Ceramics International</i> , <b>2017</b> , 43, 16531-16538	5.1	13
222	Origin of colossal dielectric response in (In + Nb) co-doped TiO rutile ceramics: a potential electrothermal material. <b>2017</b> , 7, 10144		12



221	Dielectric properties of niobium-based oxide. <i>Journal of Alloys and Compounds</i> , <b>2017</b> , 725, 342-348	5.7	10
220	Studies on dielectric, optical, magnetic, magnetic domain structure, and resistance switching characteristics of highly c-axis oriented NZFO thin films. <i>Journal of Applied Physics</i> , <b>2017</b> , 122, 033902	2.5	12
219	Nanosize effect: Enhanced compensation temperature and existence of magnetodielectric coupling in SmFeO <sub>3</sub> . <i>Physical Review B</i> , <b>2017</b> , 96,	3.3	31
218	Extrinsic contributions to the dielectric response in sintered BaTiO <sub>3</sub> nanostructures in paraelectric and ferroelectric regimes. <i>Physica B: Condensed Matter</i> , <b>2017</b> , 525, 70-77	2.8	2
217	Unusual ferroelectric and magnetic phases in multiferroic 2HBaMnO <sub>3</sub> ceramics. <i>Physical Review B</i> , <b>2017</b> , 95,	3.3	6
216	Dielectric study on mixtures of ionic liquids. <b>2017</b> , 7, 7463		18
215	Low temperature sintered giant dielectric permittivity CaCu <sub>3</sub> Ti <sub>4</sub> O <sub>12</sub> sol-gel synthesized nanoparticle capacitors. <b>2017</b> , 07, 1750017		6
214	Anisotropic percolation conduction in elastomer-carbon black composites investigated by polarization-sensitive terahertz time-domain spectroscopy. <b>2017</b> , 111, 221902		9
213	Magnetic order and magnetoelectric properties of R <sub>2</sub> CoMnO <sub>6</sub> perovskites (R=Ho, Tm, Yb, and Lu). <i>Physical Review B</i> , <b>2017</b> , 96,	3.3	33
212	Effect of Mn doping on dielectric response and optical band gap of LaGaO <sub>3</sub> . <b>2017</b> , 3, 539-549		2
211	Composite ceramics for power beaming. <b>2017</b> ,		6
210	Giant dielectric constant phenomena in Bi <sub>2</sub> O <sub>3</sub> -doped Ba <sub>0.8</sub> Sr <sub>0.2</sub> TiO <sub>3</sub> ferroelectrics. <b>2017</b> , 32, 321-326		3
209	On the multiferroic skyrmion-host GaV <sub>4</sub> S <sub>8</sub> . <b>2017</b> , 97, 3428-3445		32
208	Dielectric relaxation and ac conductivity behavior of carboxyl functionalized multiwalled carbon nanotubes/poly (vinyl alcohol) composites. <b>2017</b> , 87, 317-326		17
207	Magnetodielectric coupling in multiferroic holmium iron garnets. <i>Journal of Magnetism and Magnetic Materials</i> , <b>2017</b> , 423, 39-45	2.8	8
206	Compositionally graded ferroelectrics as wide band gap semiconductors: Electrical domain structures and the origin of low dielectric loss. <b>2017</b> , 122, 266-276		21
205	Dielectric, modulus and impedance analysis of (Ba <sub>0.9</sub> Bi <sub>0.1</sub> )(Ti <sub>0.9</sub> Al <sub>0.1</sub> )O <sub>3</sub> ceramics. <i>Journal of Materials Science: Materials in Electronics</i> , <b>2017</b> , 28, 4245-4252	2.1	3
204	Electrical conductivity and dielectric relaxation of cerium (IV) oxide. <i>Journal of Materials Science: Materials in Electronics</i> , <b>2017</b> , 28, 1501-1507	2.1	8

203	Thermal excitation contribution into the electromechanical performance of self-supported Gd-doped ceria membranes. <b>2017</b> , 256, 012008		1
202	Hysteresis Behavior of the Magnetodielectric Effect in MnZn Ferrite. <b>2018</b> , 255, 1700551		1
201	Non-Ohmic properties of MgTiO <sub>3</sub> doped CaCu <sub>3</sub> Ti <sub>4</sub> O <sub>12</sub> thin films deposited by magnetron sputtering method. <i>Journal of Alloys and Compounds</i> , <b>2018</b> , 743, 570-575	5.7	12
200	Direct Correlations of Grain Boundary Potentials to Chemical States and Dielectric Properties of Doped CaCuTiO Thin Films. <b>2018</b> , 10, 16203-16209		9
199	Disappearance of dielectric anomaly in spite of presence of structural phase transition in reduced BaTiO <sub>3</sub> : Effect of defect states within the bandgap. <i>Journal of Applied Physics</i> , <b>2018</b> , 123, 161424	2.5	27
198	Hybrid cluster precursors of the LaZrO insulator for transistors: lowering the processing temperature. <b>2018</b> , 8, 5934		5
197	Colossal dielectric behavior and relaxation in Nd-doped BaTiO <sub>3</sub> at low temperature. <i>Ceramics International</i> , <b>2018</b> , 44, 7251-7258	5.1	24
196	Effects of oxygen deficiency on the transport and dielectric properties of NdSrNbO. <b>2018</b> , 117, 1-12		25
195	Role of ytterbium on structural and magnetic properties of NiCr <sub>0.1</sub> Fe <sub>1.9</sub> O <sub>4</sub> co-precipitated ferrites. <i>Ceramics International</i> , <b>2018</b> , 44, 5433-5439	5.1	11
194	Study of proton-conducting polymer electrolyte based on K-carrageenan and NH <sub>4</sub> SCN for electrochemical devices. <b>2018</b> , 24, 3535-3542		24
193	Impact of post-deposition annealing on RF sputtered calcium copper titanate thin film for memory application. <b>2018</b> , 5, 074001		3
192	High dielectric and actuated properties of silicone dielectric elastomers filled with magnesium-doped calcium copper titanate particles. <b>2018</b> , 39, 691-697		20
191	Structural, electrical, optical and dielectric properties of sol-gel derived (1-x) BiFeO <sub>3</sub> [(x) Pb(Zr <sub>0.52</sub> Ti <sub>0.48</sub> )O <sub>3</sub> ] novel multiferroics materials. <i>Journal of Alloys and Compounds</i> , <b>2018</b> , 732, 666-673	5.7	16
190	Structural, thermal, dielectric and ferroelectric properties of K <sub>0.5</sub> Bi <sub>0.5</sub> TiO <sub>3</sub> ceramics. <b>2018</b> , 38, 567-574		22
189	Giant dielectric permittivity and magneto-capacitance effect in YBaCuFeO <sub>5</sub> . <b>2018</b> , 146, 160-163		6
188	Conductivity relaxation in Pb <sub>0.9</sub> Sm <sub>0.1</sub> Zr <sub>0.405</sub> Ti <sub>0.495</sub> Fe <sub>0.1</sub> O <sub>3</sub> solid solution. <i>Journal of Alloys and Compounds</i> , <b>2018</b> , 735, 1472-1479	5.7	9
187	Semiconductor Effects in Ferroelectrics. <b>2018</b> , 97-178		2
186	Thickness Dependence of Photoconductance in Strained BiFeO <sub>3</sub> Thin Films With Planar Device Geometry. <b>2018</b> , 12, 1700301		4

185	Dielectric studies of CCTO-based nanocomposite ceramic synthesized by a solid state route. <b>2018</b> , 109, 916-921		2
184	Colossal dielectric permittivity in Co-doped ZnO ceramics prepared by a pressure-less sintering method. <b>2018</b> , 20, 28712-28719		14
183	Orbital-order driven ferroelectricity and dipolar relaxation dynamics in multiferroic GaMo4S8. <i>Physical Review B</i> , <b>2018</b> , 98,	3-3	14
182	The effect of film/electrode interfaces on the dielectric responses of highly (000l)-oriented M-type BaFe12O19 thin films synthesized using chemical solution deposition. <b>2018</b> , 113, 262902		2
181	Dielectric Properties of Confined Ionic Liquids. <i>Ceramic Transactions</i> , <b>2018</b> , 191-199		0.1
180	Dielectric properties of ferromagnetic Ni nanoparticles added (Cu0.5Ti0.5)Ba2Ca2Cu3O10- $\delta$ superconducting phase. <b>2018</b> , 44, 759-764		
179	Study of structural, morphological, optical, and dielectric behaviour of zinc-doped nanocrystalline lanthanum chromite. <i>Applied Physics A: Materials Science and Processing</i> , <b>2018</b> , 124, 1	2.6	9
178	Magnetoresistance, magnetic, and dielectric properties of LuFe2O4 prepared by ebeam-assisted solid state reaction. <i>Journal of Applied Physics</i> , <b>2018</b> , 124, 144101	2.5	4
177	Dielectric and impedance studies of La and Zn co-doped complex perovskite CaCu3Ti4O12 ceramic. <i>Ceramics International</i> , <b>2018</b> , 44, 23125-23136	5.1	29
176	Thermal behavior and properties of CaCu3Ti4O12 ceramic synthesized by organo-metallic compound. <i>Applied Physics A: Materials Science and Processing</i> , <b>2018</b> , 124, 1	2.6	1
175	Significance of in-plane oxygen vacancy rich non-stoichiometric layer towards unusual high dielectric constant in nano-structured SnO2. <b>2018</b> , 103, 60-65		13
174	A giant 2-dimensional dielectric response in a compressed hydrogen-bonded hybrid organic/inorganic salt. <b>2018</b> , 6, 7689-7699		11
173	References. <b>2018</b> , 481-515		
172	Polymer-based nanocomposites for significantly enhanced dielectric properties and energy storage capability. <b>2018</b> , 131-183		
171	Numerical model for the characterization of Maxwell-Wagner relaxation in piezoelectric and flexoelectric composite material. <b>2018</b> , 208, 75-91		25
170	Frequency dependent polarisation switching in h-ErMnO3. <b>2018</b> , 112, 182908		20
169	Cellulose nanofibrils-reduced graphene oxide xerogels and cryogels for dielectric and electrochemical storage applications. <b>2018</b> , 147, 260-270		34
168	Magnetic field tunable dielectric dispersion in successive field-induced magnetic phases of the geometrically frustrated magnet CuFeO2 up to 28 T. <i>Physical Review B</i> , <b>2018</b> , 97,	3-3	2

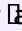
167	In situ synthesized SrF <sub>2</sub> /polyvinylidene fluoride nanocomposite film based photo-power cell with imperious performance and stability. <b>2018</b> , 282, 194-204		5
166	Characterization of multiferroic PbFe <sub>0.5</sub> Nb <sub>0.5</sub> O <sub>3</sub> and PbFe <sub>0.5</sub> Ta <sub>0.5</sub> O <sub>3</sub> ceramics derived from citrate polymeric precursors. <i>Journal of the American Ceramic Society</i> , <b>2019</b> , 102, 1296-1308	3.8	7
165	Structure and Enhanced Dielectric Properties of B and Sr Modified CaCu <sub>3</sub> Ti <sub>4</sub> O <sub>12</sub> Ceramics. <b>2019</b> , 48, 6354-6358		5
164	Magnetic and electrical transport properties of YbFe <sub>2</sub> O <sub>4</sub> . <i>Physical Review B</i> , <b>2019</b> , 100,	3.3	3
163	Nano-manipulation and nano-assembling using shape memory alloy nanogripper of metal oxide and semiconductor single nanowires and nanoparticles for biological nanosensors. <b>2019</b> , 10, 035003		3
162	Sintering temperature effects on some physical properties of a Dy <sub>0.5</sub> (Sr/Ca) <sub>0.5</sub> MnO <sub>3</sub> system. <b>2019</b> , 134, 1		2
161	Spin ordering and physical properties of NaPrFeWO <sub>6</sub> and NaSmFeWO <sub>6</sub> with polar double perovskite structure. <b>2019</b> , 176, 53-62		5
160	Dielectric dispersion in pure, samarium, samarium & tin doped potassium niobate single crystals. <b>2019</b> , 540, 54-64		1
159	Ferroelectric polarization in multiferroics. <b>2019</b> , 4,		2
158	Phase Cu-Phthalocyanine/Acrylonitrile Butadiene Styrene Terpolymer Nanocomposite Film Technology for Organoelectronic Applications. <b>2019</b> , 123, 28081-28092		17
157	The effect of Sr doping on structural and dielectric properties of Ba <sub>2</sub> Co <sub>2</sub> Fe <sub>12</sub> O <sub>22</sub> ceramics. <i>Journal of Materials Science: Materials in Electronics</i> , <b>2019</b> , 30, 21079-21088	2.1	1
156	High-Pressure Synthesis and Ferrimagnetism of NiTeO-Type MnScMO (M = Nb, Ta). <b>2019</b> , 58, 15953-15961		3
155	Photo-charging polymeric sodium-ion cell based on YSZ/PVDF film. <b>2019</b> , 115, 183904		2
154	Electrical response of mixed phase (1-x)BiFeO <sub>3</sub> -xPbTiO <sub>3</sub> solid solution: Role of tetragonal phase and tetragonality. <i>Journal of Alloys and Compounds</i> , <b>2019</b> , 786, 98-108	5.7	8
153	Magneto-dielectric and multiferroic properties in Bi <sub>0.95</sub> Yb <sub>0.05</sub> Fe <sub>0.95</sub> Co <sub>0.05</sub> O <sub>3</sub> . <b>2019</b> , 94, 065802		6
152	Impact of crystal stacking sequence on electrical transport and dielectric properties of the nanocrystalline BaCo <sub>0.9</sub> Mn <sub>0.1</sub> O <sub>3</sub> . <i>Journal of Alloys and Compounds</i> , <b>2019</b> , 786, 356-367	5.7	7
151	Influence of chemical substitution on broadband dielectric response of barium-lead M-type hexaferrite. <b>2019</b> , 21, 063016		16
150	Dielectric, pyroelectric and polarization behavior of polyvinylidene fluoride (PVDF) - Gold nanoparticles (AuNPs) nanocomposites. <b>2019</b> , 166, 298-306		8

149	Effect of neodymium doping on electrical properties and relaxor ferroelectric behavior of YCrO <sub>3</sub> nanoparticles. <b>2019</b> , 113, 194-201		6
148	Large positive magnetoconductivity at microwave frequencies in the compensated topological insulator BiSbTeSe <sub>2</sub> . <i>Physical Review B</i> , <b>2019</b> , 99,	3-3	2
147	Observation of both debye type and Maxwell-Wagner relaxation in Y <sub>1.9</sub> Ce <sub>0.1</sub> CoMnO <sub>6</sub> . <b>2019</b> ,		
146	Electrospun Spandex Nanofiber Webs with Ionic Liquid for Highly Sensitive, Low Hysteresis Piezocapacitive Sensor. <b>2019</b> , 20, 337-347		10
145	Non-Ohmic behavior of copper-rich CCTO thin film prepared through magnetron sputtering method. <i>Journal of Materials Science: Materials in Electronics</i> , <b>2019</b> , 30, 9266-9272	2-1	2
144	Colossal Permittivity Materials as Superior Dielectrics for Diverse Applications. <b>2019</b> , 29, 1808118		67
143	Dielectric Properties of Polytetrafluoroethylene/CaCu <sub>3</sub> Ti <sub>4</sub> O <sub>12</sub> Composites. <b>2019</b> , 34, 189-194		5
142	Temperature dependent conductivity mechanisms observed in Pr <sub>2</sub> NiTiO <sub>6</sub> . <i>Materials Chemistry and Physics</i> , <b>2019</b> , 230, 277-286	4-4	7
141	Titanium-Based Dual-function Varistor Ceramics. <b>2019</b> , 335-406		
140	Dielectric relaxations in fine-grained SrTiO <sub>3</sub> ceramics with Cu and Nb co-doping. <i>Ceramics International</i> , <b>2019</b> , 45, 10334-10341	5-1	13
139	Intrinsic Ferroelectricity in Charge-Ordered Magnetite. <b>2019</b> , 9, 546		0
138	Electrical transport properties of Ni-doped diamond-like carbon films at and above room temperature. <i>Journal of Applied Physics</i> , <b>2019</b> , 126, 154104	2-5	4
137	Improved uniaxial dielectric properties in aligned diisopropylammonium bromide (DIPAB) doped poly(vinylidene difluoride) (PVDF) nanofibers.. <b>2019</b> , 9, 31233-31240		4
136	Variable-range-hopping conduction and polaron dielectric relaxation in Cu and Nb co-doped BaTiO <sub>3</sub> . <b>2019</b> , 129, 111-121		10
135	Impact of low titanium concentration on the structural, electrical and dielectric properties of Pr <sub>0.75</sub> Bi <sub>0.05</sub> Sr <sub>0.1</sub> Ba <sub>0.1</sub> Mn <sub>1-x</sub> Ti <sub>x</sub> O <sub>3</sub> (x = 0, 0.04) compounds. <i>Journal of Materials Science: Materials in Electronics</i> , <b>2019</b> , 30, 876-891	2-1	16
134	Impact of silver dopant on electrical and dielectric properties of ZnO nanoparticles. <b>2019</b> , 6, 035014		7
133	Reversible Structural Transformation between Polar Polymorphs of LiGeTeO. <b>2019</b> , 58, 1599-1606		4
132	Sol-gel derived cobalt doped LaCrO <sub>3</sub> : Structure and physical properties. <i>Journal of Alloys and Compounds</i> , <b>2019</b> , 784, 541-555	5-7	31

131	Low temperature magneto-dielectric coupling in nanoscale layered $\text{SmFe}_{0.5}\text{Co}_{0.5}\text{O}_3$ perovskite. <b>2019</b> , 127, 164-168		5
130	Enhanced dielectric properties and electrical responses of cobalt-doped $\text{CaCu}_3\text{Ti}_4\text{O}_{12}$ thin films. <i>Journal of Alloys and Compounds</i> , <b>2019</b> , 773, 853-859	5-7	54
129	Contribution of nanointerfaces to colossal permittivity of doped $\text{Ba}(\text{Ti},\text{Sn})\text{O}_3$ ceramics. <b>2019</b> , 9, 767-773		1
128	Effect of synthesis method on magnetic and dielectric properties of $\text{CuBO}_2$ delafossite oxide. <b>2020</b> , 56, 499-505		1
127	Dielectric and conductivity investigation of polycarbonate-copper phthalocyanine electrospun nonwoven fibres for electrical and electronic application. <b>2020</b> , 59, 154-168		16
126	Deep trap states relaxation in $\text{CaCu}_3\text{Ti}_4\text{O}_{12}$ . <i>Journal of Alloys and Compounds</i> , <b>2020</b> , 814, 152185	5-7	2
125	Improvement in varistor properties of $\text{CaCu}_3\text{Ti}_4\text{O}_{12}$ ceramics by chromium addition. <b>2020</b> , 41, 12-20		19
124	Influence of oxygen deficiency on optical and dielectric properties of $\text{La}_{0.75}\text{Ba}_{0.10}\text{Sr}_{0.15}\text{FeO}_{2.875-x}$ compounds. <b>2020</b> , 741, 137106		1
123	AC-conduction mechanism via dielectric measurements of $(\text{Cr})_x/(\text{CuTi})$ -1223 nanoparticles-superconductor composites. <b>2020</b> , 105, 103021		5
122	Local control of improper ferroelectric domains in $\text{YMnO}_3$ . <i>Physical Review B</i> , <b>2020</b> , 102,	3-3	5
121	Antisite disorder driven magnetodielectric and magnetocaloric effect in double perovskite $\text{La}_{2-x}\text{Sr}_x\text{CoMnO}_6$ ( $x = 0.0, 0.5, 1.0$ ). <i>Journal of Applied Physics</i> , <b>2020</b> , 128, 024104	2-5	3
120	Effect of cation arrangement on polaron formation and colossal permittivity in $\text{NiNb}_2\text{O}_6$ . <b>2020</b> , 8, 16107-16112		1
119	Anomalous conductivity behavior induced by in situ metastable amorphous phase in $\text{BaTiO}_3/\text{Ni}_{0.5}\text{Zn}_{0.5}\text{Fe}_2\text{O}_4$ ceramic composite. <i>Ceramics International</i> , <b>2020</b> , 46, 28659-28667	5-1	1
118	Effects of sintering temperature on structural, electrical and ferroelectric properties of $\text{La}_2\text{Ti}_2\text{O}_7$ ceramics. <i>Ceramics International</i> , <b>2020</b> , 46, 26790-26799	5-1	5
117	Structural, magnetic and electrical characterization of Cr-doped lead-free multiferroic $\text{AlFeO}_3$ prepared by co-precipitation and solid state method. <b>2020</b> , 34, 2050183		0
116	Colossal dielectric response, relaxation mechanism and multiferroic properties of $(\text{Ba}_{1-x}\text{Sm}_x)(\text{Ti}_{1-x}\text{Fe}_x)\text{O}_3$ ( $0.0 \leq x \leq 0.5$ ). <b>2020</b> , 260, 114624		1
115	Role of aromatic aliphatic amine for the variation of structural, electrical and catalytic behaviors in a series of silver phosphonate extended hybrid solids. <b>2020</b> , 49, 13618-13634		7
114	Probing insulators under pressure. <i>Review of Scientific Instruments</i> , <b>2020</b> , 91, 093902	1-7	1

113	Equivalent circuit modeling on defect-dipole enhanced dielectric permittivity. <b>2020</b> , 8, 13235-13243		6
112	A New Approach to the Fabrication of Memristive Neuromorphic Devices: Compositionally Graded Films. <b>2020</b> , 13,		1
111	Glassy dielectric anomaly and negative magneto-capacitance effect in electron-doped $\text{Ca}_{1-x}\text{Sr}_x\text{Mn}_{0.85}\text{Sb}_{0.15}\text{O}_3$ . <i>Journal of Applied Physics</i> , <b>2020</b> , 127, 184105	2.5	2
110	New approach for synthesis of nano-sized $\text{CaCu}_3\text{Ti}_4\text{O}_{12}$ powder by economic and innovative method. <i>Journal of Materials Science: Materials in Electronics</i> , <b>2020</b> , 31, 9065-9075	2.1	4
109	Dielectric relaxation, magneto-dielectric coupling, and pyrocurrent anomaly in point defect controlled $\text{HoCrO}_3$ . <i>Journal of Applied Physics</i> , <b>2020</b> , 127, 194105	2.5	0
108	Synthesis Dependent Structural Magnetic and Electrical Properties of CR-Doped Lead-Free Multiferroic $\text{AlFeO}_3$ . <b>2020</b> , 10, 440		0
107	Tailoring the electrical conductivity and hardening in $\text{BiFeO}_3$ ceramics. <b>2020</b> , 40, 5483-5493		6
106	Effects of defect dipoles on the colossal permittivity of ambipolar co-doped rutile $\text{TiO}_2$ ceramics. <b>2020</b> , 143, 109456		2
105	Nonvolatile Negative Optoelectronic Memory Based on Ferroelectric Thin Films. <b>2020</b> , 2, 1035-1040		9
104	Ruddlesden-Popper phase $\text{A}_2\text{BO}_4$ oxides: Recent studies on structure, electrical, dielectric, and optical properties. <b>2020</b> , 9, 129-148		34
103	Double pentavalent ( $\text{Sb}^{5+}$ , $\text{Nb}^{5+}$ ) and trivalent ( $\text{Sm}^{3+}$ , $\text{Y}^{3+}$ ) co-doped $\text{Ti}_{0.9}\text{Zr}_{0.1}\text{O}_2$ colossal dielectric permittivity multilayer ceramics for the miniaturization of the next-generation electronics. <i>Ceramics International</i> , <b>2020</b> , 46, 23433-23441	5.1	2
102	Colossal Dielectric Responses from the Wide Band Gap 2D-Semiconducting Amine Templated Hybrid Framework Materials. <b>2020</b> , 59, 9465-9470		4
101	High-transconductance indium oxide transistors with a lanthanum-zirconium gate oxide characteristic of an electrolyte. <i>Journal of Applied Physics</i> , <b>2020</b> , 127, 064504	2.5	1
100	Enhancement of breakdown electric field and dielectric properties of $\text{CaCu}_3\text{Ti}_4\text{O}_{12}$ ceramics by Sr doping. <i>Materials Chemistry and Physics</i> , <b>2020</b> , 244, 122722	4.4	10
99	Unexpected Giant Microwave Conductivity in a Nominally Silent $\text{BiFeO}_3$ Domain Wall. <b>2020</b> , 32, e1905132		11
98	Enhanced dielectric properties and grain boundary potentials in sulfur-doped $\text{CaCu}_3\text{Ti}_4\text{O}_{12}$ thin films. <b>2020</b> , 40, 2375-2381		2
97	Charge transport by global protonic conductivity and relaxational dynamics over hydrogen bonds in $\text{Fe}_2+\text{Fe}_3+3.2(\text{Mn}^{2+},\text{Zn})_{0.8}(\text{PO}_4)_3(\text{OH})_{4.2}(\text{HOH})_{0.8}$ . <b>2020</b> , 347, 115240		2
96	Electronic structure and intrinsic dielectric polarization of defect-engineered rutile $\text{TiO}_2$ . <b>2021</b> , 9, 595-599		3



95	Variable range hopping and modulus relaxation in NiFe <sub>2</sub> O <sub>4</sub> ceramics. <i>Materials Chemistry and Physics</i> , <b>2021</b> , 259, 124135	4.4	4
94	Synthesis of the hollandite-like copper doped potassium titanate high-k ceramics. <i>Ceramics International</i> , <b>2021</b> , 47, 5721-5729	5.1	9
93	Improved energy storage capacity in strontium and manganese co-doped 0.925(Bi <sup>1/2</sup> Na <sup>1/2</sup> )TiO <sub>3</sub> -0.075BaTiO <sub>3</sub> ceramics. <b>2021</b> , 263, 114869		0
92	Dielectric Relaxation Mechanism in High-Pressure Synthesized BiCr <sub>0.5</sub> Mn <sub>0.5</sub> O <sub>3</sub> . <b>2021</b> , 50, 1615-1620		1
91	The Interaction of Electromagnetic Waves with Ice. <b>2021</b> , 105-129		
90	The Interaction of Electromagnetic Waves with Water. <b>2021</b> , 51-104		
89	Insulating improper ferroelectric domain walls as robust barrier layer capacitors. <i>Journal of Applied Physics</i> , <b>2021</b> , 129, 074101	2.5	5
88	High dielectric thin films based on UV-reduced graphene oxide and TEMPO-oxidized cellulose nanofibres. <b>2021</b> , 28, 3069-3080		3
87	Entropy stabilized multicomponent oxides with diverse functionality  review. 1-52		6
86	Charge carrier confinement in hematite and hematite / MoTe <sub>2</sub> nanocomposites; the role of interface states. <b>2021</b> , 113, 106532		1
85	Signatures of spin-phonon coupling in hematite crystallites through dielectric and Raman spectroscopy. <b>2021</b> , 134, 47003		2
84	Cooperative Cluster Jahn-Teller Effect as a Possible Route to Antiferroelectricity. <b>2021</b> , 126, 187601		6
83	High temperature impedance spectroscopy study of KTaO <sub>3</sub> (001) single crystal. <i>Journal of Alloys and Compounds</i> , <b>2021</b> , 863, 158317	5.7	0
82	A structural perspective on giant permittivity CaCu <sub>3</sub> Ti <sub>4</sub> O <sub>12</sub> : One way to quantum dielectric physics in solids. <b>2021</b> , 6, 100126		2
81	Enhancement of dielectric response by the interaction of point defect and grain boundary in copper tantalate oxides. <i>Ceramics International</i> , <b>2021</b> , 47, 16178-16185	5.1	1
80	Dynamical response of localized electron hopping and dipole relaxation in Cu <sub>1-x</sub> Zn <sub>x</sub> Fe <sub>2</sub> O <sub>4</sub> magnetoceramics.		0
79	Piezoelectric Nonlinearity and Hysteresis Arising from Dynamics of Electrically Conducting Domain Walls.		
78	Structure-dependent dielectric relaxations in Sm-doped BaTiO <sub>3</sub> ceramics. <i>Ceramics International</i> , <b>2021</b> , 47, 34042-34042	5.1	0



77	Nanostructured multiferroic Pb(Zr,Ti)O <sub>3</sub> /NiFe <sub>2</sub> O <sub>4</sub> thin-film composites. <i>Thin Solid Films</i> , <b>2021</b> , 732, 1387402		
76	Analysis of the electrical transport, conductivity, and dielectric relaxation behavior of La <sub>0.75</sub> Ba <sub>0.10</sub> Sr <sub>0.15</sub> Fe O <sub>2.875-<math>\Gamma</math></sub> (x= 0.375 and 0.50) brownmillerite oxides. <i>Journal of Materials Science: Materials in Electronics</i> , <b>2021</b> , 32, 21897-21908	2.1	
75	On the complexity of spinels: Magnetic, electronic, and polar ground states. <i>Physics Reports</i> , <b>2021</b> , 926, 1-86	27.7	12
74	Anomalous structural behavior and antiferroelectricity in BiGdO: detailed temperature and high-pressure study. <i>Journal of Physics Condensed Matter</i> , <b>2021</b> , 33,	1.8	1
73	Synthesis, structural characterization, electric and dielectric properties of Pr <sub>0.67</sub> Ba <sub>0.22</sub> Sr <sub>0.11</sub> Mn <sub>0.925</sub> Ni <sub>0.075</sub> O <sub>3</sub> perovskite for thermal energy storage. <i>Journal of Alloys and Compounds</i> , <b>2021</b> , 874, 159866	5.7	1
72	Giant caloric effects close to any critical end point. <i>Materials Research Bulletin</i> , <b>2021</b> , 142, 111413	5.1	3
71	Broadband Dielectric Spectroscopy A Practical Guide. <i>ACS Symposium Series</i> , <b>2021</b> , 3-59	0.4	4
70	Equivalent Circuit Modeling of Core-Shell Structured Ceramic Materials. <i>Ceramic Transactions</i> , 23-29	0.1	5
69	Chapter 3:Characterization of Capacitance, Transport and Recombination Parameters in Hybrid Perovskite and Organic Solar Cells. <i>RSC Energy and Environment Series</i> , <b>2016</b> , 57-106	0.6	7
68	Charge transport in oxygen-deficient EuTiO <sub>3</sub> : The emerging picture of dilute metallicity in quantum-paraelectric perovskite oxides. <i>Physical Review Materials</i> , <b>2019</b> , 3,	3.2	8
67	Dielectric properties of CaCu <sub>3-x</sub> Mg <sub>x</sub> Ti <sub>4</sub> O <sub>12</sub> (x=0.20 and 0.50) material synthesized by the semi-wet route for energy storage capacitor. <b>2019</b> ,		1
66	Semiconducting Properties of Cu <sub>5</sub> SbO <sub>6</sub> . <i>Acta Physica Polonica A</i> , <b>2012</b> , 122, 1105-1107	0.6	1
65	The effect of Nd doping on microstructure and electrical properties of BiFeO <sub>3</sub> thin films. <i>Hongwai Yu Haomibo Xuebao/Journal of Infrared and Millimeter Waves</i> , <b>2012</b> , 31, 21-25	0	2
64	Complex Conductivity Using Wideband Spectroscopy for Yttria/Ytterbia-Stabilized Zirconia Ceramics. <i>Japanese Journal of Applied Physics</i> , <b>2012</b> , 51, 011102	1.4	8
63	Innovative non-thermal plasma coating for core-shell CaCu <sub>3</sub> Ti <sub>4</sub> O <sub>12</sub> material. <i>Journal of Applied Physics</i> , <b>2021</b> , 130, 163305	2.5	
62	Colossal Permittivity in Advanced Functional Heterogeneous Materials: The Relevance of the Local Measurements at Submicron Scale. <i>Nanoscience and Technology</i> , <b>2010</b> , 613-646	0.6	
61	Electronic Properties of BaTiO <sub>3</sub> Containing Glass Ceramics. <i>Ceramic Transactions</i> , 65-72	0.1	
60	Effects of Pr Substitution on Electrical Properties of Bi(Fe <sub>0.95</sub> Mn <sub>0.05</sub> )O <sub>3</sub> Thin Films. <i>Japanese Journal of Applied Physics</i> , <b>2011</b> , 50, 01BF07	1.4	

59	Anisotropic Colossal Dielectric Response of $0.93\text{Pb}(\text{Fe}_{1/2}\text{Nb}_{1/2})\text{O}_3\text{-}0.07\text{PbTiO}_3$ Single Crystals along [100] and [111] Directions. <i>Japanese Journal of Applied Physics</i> , <b>2011</b> , 50, 101502	1.4	
58	The Varistor Property of $\text{SnO}_2\text{-Zn}_2\text{SnO}_4$ Composite Ceramics. <i>Material Sciences</i> , <b>2015</b> , 05, 219-226	0.1	1
57	Dielectric and Electrical Properties of Undoped and Fe-Doped Yttrium Copper Titanate. <i>Ceramic Transactions</i> , 95-106	0.1	2
56	7: Impedance and Capacitance Spectroscopies. <b>2017</b> , 131-158		
55	Effect of $\text{Nd}^{3+}$ Doping on Magnetic and Dielectric Properties of $\text{SrFe}_{12}\text{O}_{19}$ Hexaferrite Synthesized by Coprecipitation Method. <i>Acta Physica Polonica A</i> , <b>2018</b> , 133, 669-672	0.6	1
54	Improvement of Solid Through Improved Solutions and Gels (2): The Other Methods. <b>2019</b> , 277-308		
53	Charged Ferroelectric Domain Walls for Deterministic ac Signal Control at the Nanoscale. <i>Nano Letters</i> , <b>2021</b> , 21, 9560-9566	11.5	4
52	The enhanced cutoff frequency of dielectric constant for K-doped $\text{Na}_{0.5}\text{Y}_{0.5}\text{Cu}_3\text{Ti}_4\text{O}_{12}$ ceramics. <i>Materials Chemistry and Physics</i> , <b>2022</b> , 277, 125500	4.4	1
51	Impedance Spectroscopy of Metal Halide Perovskite Solar Cells from the Perspective of Equivalent Circuits. <i>Chemical Reviews</i> , <b>2021</b> , 121, 14430-14484	68.1	23
50	Ionic/Electronic Conduction and Capacitance of Halide Perovskite Materials. <b>2022</b> , 173-213		
49	Physical properties and structure of mechanically activated solid solution $\text{Pb}(\text{Zr}_{0.7}\text{Ti}_{0.3})\text{O}_3$ . <i>Applied Physics A: Materials Science and Processing</i> , <b>2022</b> , 128, 1	2.6	0
48	Elaboration, characterization, and giant dielectric permittivity in solid state synthesized Fe half-doped $\text{LaCrO}_3$ perovskite. <i>Materials Today: Proceedings</i> , <b>2022</b> ,	1.4	0
47	Influence of heating modes on the microstructural and dielectric properties of calcium copper titanium oxide ( $\text{CaCu}_3\text{Ti}_4\text{O}_{12}/\text{CCTO}$ ) using conventional and microwave sintering. <i>Journal of Materials Science: Materials in Electronics</i> , <b>2022</b> , 33, 5806	2.1	2
46	Synthesis and electric properties of the high-k ceramic composites based on potassium polytitanate modified by manganese. <i>Research on Chemical Intermediates</i> , <b>2022</b> , 48, 1227	2.8	
45	Tuning of the structural, morphological, dielectric, and magnetoresistance properties of $\text{Gd}_2\text{NiMnO}_6$ double perovskite by Ca doping. <i>Physica B: Condensed Matter</i> , <b>2022</b> , 632, 413734	2.8	0
44	Strontium doped $\text{CaCu}_3\text{Ti}_4\text{O}_{12}$ ceramics with very low dielectric loss synthesized by the sol-gel method. <i>Applied Physics A: Materials Science and Processing</i> , <b>2022</b> , 128,	2.6	1
43	Multiferroic properties and magnetoelectric coupling observed in nanocrystalline $\text{HoFeO}_3$ . <i>Journal of Alloys and Compounds</i> , <b>2022</b> , 907, 164443	5.7	0
42	Unveiling Alternating Current Electronic Properties at Ferroelectric Domain Walls. <i>Advanced Electronic Materials</i> , 2100996	6.4	1

41	Probing the dielectric behavior of lead-free BCST ceramic composite: An impedance spectroscopic approach. <i>Materials Today: Proceedings</i> , <b>2021</b> ,	1.4	
40	Giant Polarization in Nanodielectrics: (Invited Paper). <b>2021</b> ,		0
39	Automated real-time study of the defect-induced breakdown occurring on a film-electrode system under a high electric field.. <i>Review of Scientific Instruments</i> , <b>2021</b> , 92, 123906	1.7	0
38	Critical Sintering Temperature and Microwave Dielectric Properties of $\text{CaCu}_3\text{Ti}_4\text{O}_{12}$ Ceramics. <i>SSRN Electronic Journal</i> ,	1	
37	Giant Dielectric Response of Corundum Structure $\text{Fe}_{0.7}\text{Cr}_{1.3}\text{O}_3$ Nanocrystallite. <i>ECS Journal of Solid State Science and Technology</i> ,	2	
36	Features of the Conductivity of the $\text{Ag}_{1-x}\text{Mn}_x\text{Ge}_8\text{Sb}_2$ Solid Solutions. <i>Journal of Materials Science and Chemical Engineering</i> , <b>2022</b> , 10, 16-28	1.5	
35	Dielectric Study of Tetraalkylammonium and Tetraalkylphosphonium Levulinate Ionic Liquids. <i>International Journal of Molecular Sciences</i> , <b>2022</b> , 23, 5642	6.3	
34	Ion Dynamics in a Highly Compressed Solution of Tetra-Ethylammonium Tetrafluoroborate Salt in Propylene Carbonate: A Study in the Equilibrium and Glassy States. <i>SSRN Electronic Journal</i> ,	1	
33	Dielectric properties of conventional and microwave sintered Lanthanum doped $\text{CaCu}_3\text{Ti}_4\text{O}_{12}$ ceramics for high-frequency applications. <i>Ceramics International</i> , <b>2022</b> ,	5.1	1
32	Effect of Co-doping on the structural and dielectric properties of $\text{La}_{0.8}\text{K}_{0.2}\text{MnO}_3$ perovskite. <i>Physica Status Solidi (A) Applications and Materials Science</i> ,	1.6	
31	Synthesis and characterization of Ca-Less CCTO dielectric electroceramic materials. <i>AIP Conference Proceedings</i> , <b>2022</b> ,	0	
30	Dynamics of domain walls in ferroelectrics and relaxors. <i>Journal of the American Ceramic Society</i> ,	3.8	0
29	Magnetoelectric multiferroicity in a newly derived nanocomposite system of $(\text{Y}_{0.97}\text{Al}_{0.03}\text{FeO}_3)_x(\text{Bi}_{0.5}\text{Na}_{0.5})_{0.94}\text{Ba}_{0.06}\text{TiO}_3(1-x)$ [ $x=0.3, 0.5$ ]. <i>Journal of Magnetism and Magnetic Materials</i> , <b>2022</b> , 169553	2.8	1
28	Investigation of Dielectric Relaxor-Like Anomaly Behavior of Non-Ferroelectric $\text{BaZrO}_3$ Polycrystalline Ceramic. <i>SSRN Electronic Journal</i> ,	1	
27	Dynamic conductivity from audio to optical frequencies of semiconducting manganites approaching the metal-insulator transition *. <b>2006</b> , 518, 498-507		
26	Structural, morphological, electrical, and magnetic characteristics of $20\text{MnFe}_2\text{O}_4\text{-}80\text{SiO}_2$ nanocomposite synthesized by the one-pot auto-combustion route. <b>2022</b> , 128,		
25	Structural, morphological, electrical, and magnetic characteristics of $20\text{MnFe}_2\text{O}_4\text{-}80\text{SiO}_2$ nanocomposite synthesized by the one-pot auto-combustion route..		
24	Coherent Precipitates with Strong Domain Wall Pinning in Alkaline Niobate Ferroelectrics. 2202379		3

- 23 Ion dynamics in a highly compressed solution of tetra-ethylammonium [tetra-fluoroborate salt in propylene carbonate: A study in the equilibrium and glassy states. **2022**, 595, 121831
- 22 Structure, charge carrier conduction, dielectric properties and leakage current density of Dy<sub>2</sub>CoMnO<sub>6</sub> double perovskite. **2022**, 928, 167184
- 21 High Dielectric Permittivity and Low Transition Temperature of (1-x)CaTiO<sub>3</sub>-xFeTiO<sub>3</sub> Inorganic Composites (x = 0.0 to 1.0).
- 20 Magneto-Dielectric Effect in Epitaxial DyMnO<sub>3</sub> Thin Film.
- 19 Antipolar transitions in GaNb<sub>4</sub>Se<sub>8</sub> and GaTa<sub>4</sub>Se<sub>8</sub>. **2022**, 106,
- 18 Influence of donor doping on dielectric properties of calcium copper titanate ceramics. **2022**, 12, 105023
- 17 Dielectric response and density functional theory assessment of fluorinated dicationic pyridinium ionic liquids.
- 16 Exploring the dielectric and conduction characteristics of iodine substituted CaCu<sub>3</sub>Ti<sub>4</sub>O<sub>12</sub>-xI<sub>x</sub>. **2022**,
- 15 Colossal dielectric response and complex impedance analysis of LaFeO<sub>3</sub> ceramics. **2022**, 12,
- 14 High permittivity and low dielectric loss of the (Ca<sub>0.9</sub>Sr<sub>0.1</sub>)<sub>1-x</sub>La<sub>2x/3</sub>Cu<sub>3</sub>Ti<sub>4</sub>O<sub>12</sub> ceramics. **2022**,
- 13 Complementary Vanadium Dioxide Metamaterial with Enhanced Modulation Amplitude at Terahertz Frequencies. **2022**, 18,
- 12 Magnetolectric response of 3-phase (1-x)[0.7BiFeO<sub>3</sub>0.3CoFe<sub>2</sub>O<sub>4</sub>]-xPbTiO<sub>3</sub> multiferroic ceramic composites. **2023**, 129,
- 11 Permittivity Boosting by Induced Strain from Local Doping in Titanates from First Principles.
- 10 Flexible high-performance microcapacitors enabled by all-printed two-dimensional nanosheets. **2022**,
- 9 Spin-Lattice and Magnetolectric Couplings Enhanced by Orbital Degrees of Freedom in Polar Multiferroic Semiconductors. **2023**, 130,
- 8 Strong modulation effects on magnetolectric behavior of Co-ferrite nanoparticles incorporated in ZnO medium in nano-regime synthesized in chemical routes. **2023**, 129,
- 7 Effect of the electrical inhomogeneity on the magnetocapacitance sign change in the Ho<sub>x</sub>Mn<sub>1-x</sub>S semiconductors upon temperature and frequency variation. **2023**, 34,
- 6 Magnetic properties of Ba<sub>2</sub>Y<sub>1</sub>-Cu TaO<sub>6</sub>- solid solutions. **2023**, 571, 170560

- 5 On the enhanced dielectric and magnetic properties of BiFeO<sub>3</sub> ceramics sintered under meta-stable conditions. **2023**, 32, 101790 ○
- 4 Ultrahigh dielectric permittivity in oxide ceramics by hydrogenation. **2023**, 9, ○
- 3 Permittivity boosting by induced strain from local doping in titanates from first principles. **2023**, 13, ○
- 2 A Skin-Like Soft Compression Sensor for Robotic Applications. ○
- 1 Short-range magnetic correlation, metamagnetism, and coincident dielectric anomaly in Na<sub>5</sub>Co<sub>15.5</sub>Te<sub>6</sub>O<sub>36</sub>. **2023**, 107, ○